

5-aminosalicylic acid suppresses osteoarthritis through the OSCAR-PPAR γ axis

Received: 20 April 2023

Accepted: 16 January 2024

Published online: 03 February 2024

 Check for updatesJihee Kim ^{1,2,8}, Gina Ryu ^{1,8}, Jeongmin Seo ¹, Miyeon Go¹, Gyungmin Kim¹, Sol Yi¹, Suwon Kim³, Hana Lee⁴, June-Yong Lee⁵, Han Sung Kim⁴, Min-Chan Park⁶, Dong Hae Shin³, Hyunbo Shim ¹, Wankyu Kim¹ & Soo Young Lee ^{1,2,7} ✉

Osteoarthritis (OA) is a progressive and irreversible degenerative joint disease that is characterized by cartilage destruction, osteophyte formation, subchondral bone remodeling, and synovitis. Despite affecting millions of patients, effective and safe disease-modifying osteoarthritis drugs are lacking. Here we reveal an unexpected role for the small molecule 5-aminosalicylic acid (5-ASA), which is used as an anti-inflammatory drug in ulcerative colitis. We show that 5-ASA competes with extracellular-matrix collagen-II to bind to osteoclast-associated receptor (OSCAR) on chondrocytes. Intra-articular 5-ASA injections ameliorate OA generated by surgery-induced medial-meniscus destabilization in male mice. Significantly, this effect is also observed when 5-ASA was administered well after OA onset. Moreover, mice with DMM-induced OA that are treated with 5-ASA at weeks 8–11 and sacrificed at week 12 have thicker cartilage than untreated mice that were sacrificed at week 8. Mechanistically, 5-ASA reverses OSCAR-mediated transcriptional repression of PPAR γ in articular chondrocytes, thereby suppressing COX-2-related inflammation. It also improves chondrogenesis, strongly downregulates ECM catabolism, and promotes ECM anabolism. Our results suggest that 5-ASA could serve as a DMOAD.

Osteoarthritis (OA) is an age-related chronic degenerative joint disease that is characterized by cartilage destruction, osteophyte formation, subchondral-bone remodeling, and synovitis¹. Although it is the most common degenerative joint disease globally and a leading cause of disability and reduced quality-of-life in older people², therapeutic options mainly involve pain management³. Thus, disease-modifying OA drugs (DMOADs) that both halt OA progression and restore joint structures/functions are urgently needed.

An OA hallmark is progressive destruction of cartilage extracellular matrix (ECM)⁴. Normally, this ECM is respectively synthesized and destroyed by chondrocyte-derived anabolic and catabolic factors in equilibrium, resulting in cartilage homeostasis. In OA, this balance is tipped towards catabolism mediated by the matrix-metalloproteinases MMP3, MMP9, MMP13, and the aggrecanase ADAMTS^{5,6}. These degrade collagen-II and aggrecan (ACAN), whose synthesis is also downregulated in OA^{7,8}. Thus, targeting chondrocyte catabolic/

¹Department of Life Science, Ewha Womans University, Seoul, Republic of Korea. ²The Research Center for Cellular Homeostasis, Ewha Womans University, Seoul, Republic of Korea. ³Department of Pharmacy, Ewha Womans University, Seoul, Republic of Korea. ⁴Department of Biomedical Engineering, Yonsei University, Wonju, Republic of Korea. ⁵Department of Microbiology and Immunology, Institute for Immunology and Immunological Diseases, and Brain Korea 21 PLUS Project for Medical Sciences, Yonsei University College of Medicine, Seoul, Republic of Korea. ⁶Division of Rheumatology, Department of Internal Medicine, Yonsei University College of Medicine, Seoul, Republic of Korea. ⁷Multitasking Macrophage Research Center, Ewha Womans University, Seoul, Republic of Korea. ⁸These authors contributed equally: Jihee Kim, Gina Ryu. ✉e-mail: leesy@ewha.ac.kr

anabolic processes, thereby modifying cartilage-ECM structures, may yield promising OA therapies.

OSCAR is a receptor⁹ that binds to the triple-helical peptide GPOG-PAGFO of collagen-II¹⁰ via its extracellular domains^{11,12}. It is strongly expressed by osteoclasts, and its binding to collagen-II co-stimulates FcR γ , thereby upregulating signaling pathways that induce osteoclastogenesis¹³. Interestingly, we showed recently that although normal chondrocytes express OSCAR at negligible levels, they can be upregulated and may participate in OA: OA-cartilage chondrocytes express more OSCAR than normal in both mice and humans^{14,15}. Moreover, as reported in the present study, simply injecting OSCAR-expressing adenovirus (Ad-OSCAR) into naive mouse joints induced OA-like disease. We, therefore hypothesized that small molecules that block OSCAR-collagen binding could be DMOAD candidates. This was tested in the present study by screening 3287 compounds.

One of these inhibited the collagen binding of OSCAR on chondrocytes, namely, 5-aminosalicylic acid (5-ASA; also known as mesalamine or mesalazine). 5-ASA is widely used to treat inflammatory bowel diseases (IBDs)¹⁶, particularly ulcerative colitis (UC)¹⁷. We found that intra-articular (IA) 5-ASA injections significantly improved not only Ad-OSCAR-induced OA-like disease but also a classical murine model of OA, namely, surgery-induced medial-meniscus destabilization (DMM)¹⁸. Importantly, 5-ASA treatment also ameliorated DMM-induced OA when the injections started long after disease initiation. Late injections at weeks 8–11 also led to thicker cartilage compared to untreated mice that were sacrificed at week 8. Our RNA-seq, *in vitro*, and *in vivo* analyses showed that 5-ASA may improve OA via multiple molecular mechanisms. First, it upregulated PPAR γ , which inhibited the pro-inflammatory eicosanoid pathway. Second, it enhanced the chondrogenic differentiation of mesenchymal stem cells (MSCs), which could promote cartilage regeneration. Third, it upregulated cartilage-specific ECM-anabolism and downregulated ECM-catabolism. Thus, OSCAR may play a key role in OA pathogenesis and 5-ASA may have significant potential as an IA-administered DMOAD.

Results

OSCAR-overexpression in joint tissue induces cartilage degeneration

Since we found recently that OA cartilage overexpresses OSCAR^{14,15}, we asked whether overexpressing OSCAR in naive joints would induce OA. Since Ad-OSCAR infection of chondrocytes *in vitro* strongly upregulates their OSCAR expression (Fig. 1a, b) and IA-injection of recombinant adenovirus effectively delivers genes to joint tissues^{19,20}, we IA-injected murine knees with Ad-OSCAR (3 weekly injections; Fig. 1c). By the end of the third week, this induced *in vivo* chondrocyte-overexpression of OSCAR (Fig. 1d), damaged the glycosaminoglycans in the articular cartilage, and induced synovitis. Notably, there was no obvious cartilage loss or osteophyte development, and the thickening of the subchondral bone plate (SBP) that is suggestive of sclerosis was not observed (Fig. 1e, f). However, as will be detailed later, when mice were treated for 8 weeks with IA Ad-OSCAR injections, cartilage destruction, osteophyte formation, SBP thickening, and synovitis were observed (Fig. 1h, i). Nonetheless, it should be noted that the Ad-OSCAR-induced model involves OA-like disease rather than classical OA.

Conversely, knocking down OSCAR in mice that were developing DMM-induced OA significantly ameliorated OA¹⁴: joint histology at 9 weeks of mice that underwent weekly IA-injections with small-hairpin OSCAR-expressing adenovirus (Ad-shOSCAR) starting 1 week after DMM surgery revealed marked improvements in their severe cartilage destruction (as indicated by Osteoarthritis Research Society International [OARSI] grading), osteophyte maturity, SBP thickness, and synovitis. These effects depended on Ad-shOSCAR multiplicity-of-infection (MOI) (Supplementary Fig. 1). Thus, OSCAR is necessary and sufficient for the development of OA/OA-like disease.

Screening and verification of OSCAR-antagonists

The extracellular OSCAR domain binds to collagen-II via the GPOG-PAGFO consensus sequence¹⁰. Moreover, this peptide (denoted as COL^{pep}) binds both to recombinant OSCAR protein and cell-surface OSCAR on chondrocytes¹⁴. It should be noted at this point that while normal chondrocytes express OSCAR-mRNA/protein at negligible levels, we found that this expression is upregulated *in vitro* by IL-1 β ¹⁴, which stimulates chondrocytes to produce cartilage-destroying enzymes such as MMPs and aggrecanase^{6,21}. Moreover, culture of normal chondrocytes on COL^{pep}-coated plates also increases their native OSCAR transcription, and IL-1 β augments it further (Supplementary Fig. 2a). While unstimulated Ad-OSCAR-infected chondrocytes express ~300-fold more OSCAR than IL-1 β +COL^{pep}-stimulated uninfected chondrocytes (Supplementary Fig. 2b), IL-1 β and/or COL^{pep} also augment it (Supplementary Fig. 2c). These OSCAR-transcription responses reflect downstream signaling induced by COL^{pep}-bound OSCAR that triggers new OSCAR expression¹⁵. These responses served as readouts of the binding of chondrocyte-surface OSCAR to COL^{pep} in our study.

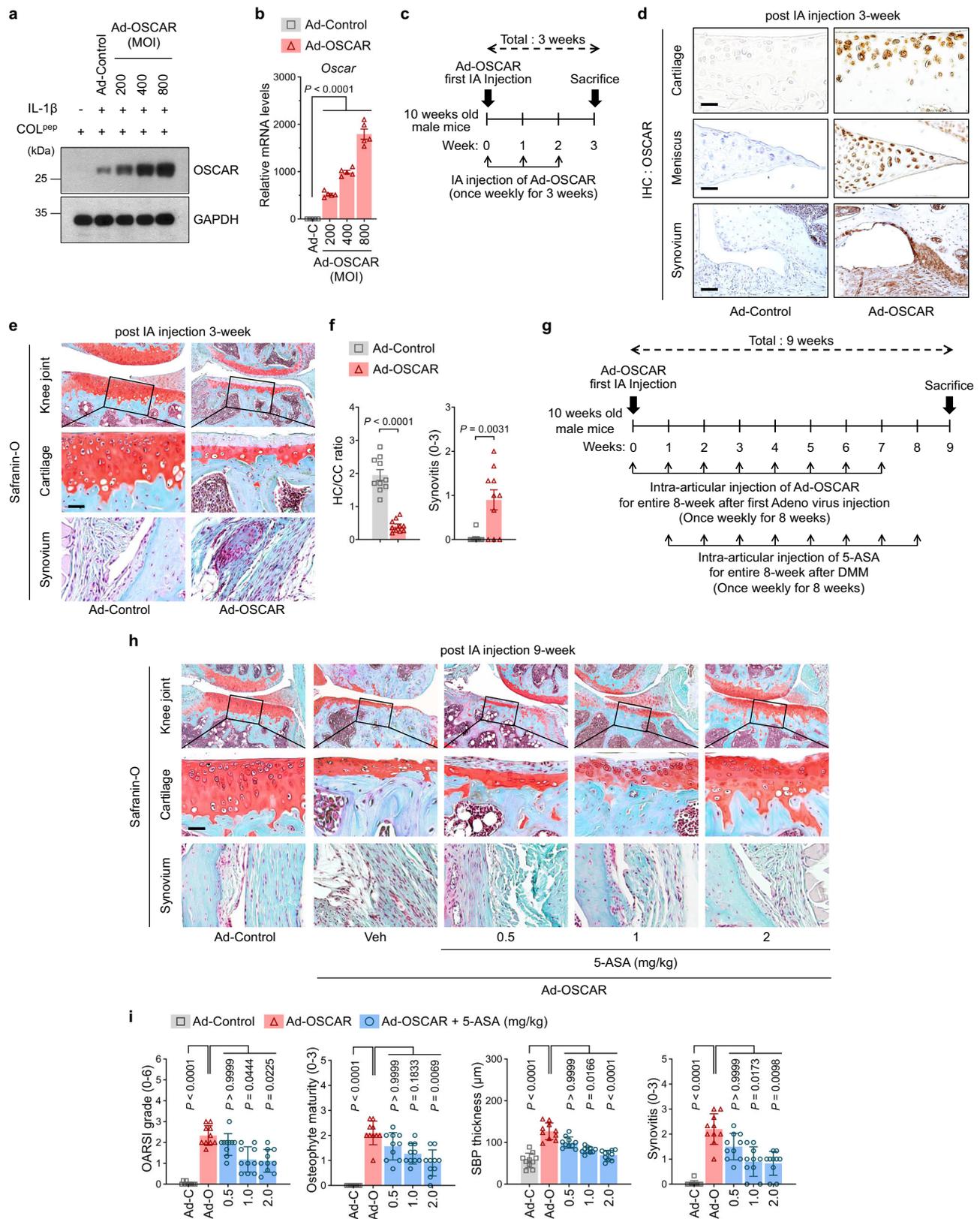
Thus, COL^{pep} was used in our ELISA-based screening system to find small molecules that structurally inhibit the collagen-II binding of OSCAR. The system uses purified hOSCAR-Fc, a fusion protein of human OSCAR and human-IgG Fc, which efficiently binds to COL^{pep} (ref. 14). The screening involved immobilizing COL^{pep}, adding hOSCAR-Fc with small molecules, and detecting disruption of hOSCAR-Fc binding to COL^{pep} (Supplementary Fig. 2d). The 3287 screened small compounds were structurally diverse and originated from a natural-compound library and an FDA-approved drug library (Supplementary Fig. 2e). Of the 165 primary target compounds that emerged, 124 compounds were excluded because their role in chondrocytes or OA has already been studied (Supplementary Fig. 2f; Supplementary Data 1). Of the 41 remaining candidates, three underwent further study because they competed with COL^{pep} most strongly (Supplementary Fig. 2g). They were epigallocatechin-3-gallate (EGCG), morin hydrate, and 5-ASA (Supplementary Fig. 2h). Dose-ELISAs confirmed that these molecules suppressed hOSCAR-Fc binding to COL^{pep} (Supplementary Fig. 3a) and 5-ASA had the lowest IC₁₀, IC₅₀ and IC₉₀ value (Supplementary Fig. 3b).

5-ASA competes with collagen-II for binding to OSCAR

Next, we asked whether the three candidate molecules could compete with COL^{pep} for binding to chondrocyte-expressed OSCAR. We thus cultured chondrocytes on COL^{pep}-coated plates, infected them with Ad-OSCAR and treated them with increasing candidate molecule concentrations. OSCAR-qRT-PCR showed that only 5-ASA downregulates COL^{pep}-induced OSCAR transcription in chondrocytes (Supplementary Fig. 3c). Since 10 μ M 5-ASA had a particularly marked effect, this concentration was used further in *in vitro* experiments.

5-ASA-mediated downregulation of OSCAR expression was also observed when OSCAR expression on normal human and murine chondrocytes was upregulated by IL-1 β +COL^{pep} treatment: 5-ASA significantly antagonized OSCAR-protein expression in this setting (Supplementary Fig. 3d). Similarly, 5-ASA antagonized the high OSCAR-protein and mRNA expression in IL-1 β +COL^{pep}-treated Ad-OSCAR-infected chondrocytes (Supplementary Fig. 3e, f). It should be noted here that since our screening ELISAs showed that 5-ASA binds directly to OSCAR, 5-ASA probably modulates OSCAR expression in chondrocytes by displacing COL^{pep} from cell-surface OSCAR, thus eliminating the downstream signaling induced by COL^{pep}-bound OSCAR that stimulates *de novo* OSCAR expression.

These results show that 5-ASA powerfully competes with OSCAR-collagen binding. Induced-fit docking (IFD) studies showed that Tyr166, Tyr200, and Ser211 in OSCAR were important for its binding to



epigallocatechin-3-gallate, morin hydrate, and 5-ASA (Supplementary Fig. 3g). More specifically, the IFD analysis showed that hOSCAR and 5-ASA likely bound stably because (i) the 5-amino and carboxylate groups of 5-ASA form hydrogen bonds with Ser211 and Tyr166 in hOSCAR-Fc, respectively; and (ii) the aromatic ring of 5-ASA interacts

with Tyr200 through π - π stacking. This was confirmed by mutating each residue in 5-ASA to alanine and conducting the COL^{PEP}/hOSCAR-Fc ELISA: each substitution abolished 5-ASA binding to OSCAR (Supplementary Fig. 3h). Thus, 5-ASA is an antagonist that binds at Y166, Y200, and S211 of OSCAR and inhibits its binding to collagen-II.

Fig. 1 | 5-ASA attenuates OA caused by OSCAR overexpression in mouse articular cartilage. **a, b** Cultured primary chondrocytes from C57BL/6J mice were infected with Ad-Control (Ad-C; 800 MOI) or the indicated MOI of Ad-OSCAR ($n = 5$). **a** Western blotting with anti-OSCAR antibody. **b** qRT-PCR analysis of OSCAR mRNA expression. **c–e** C57BL/6J mice underwent IA injections once per week for 3 weeks with Ad-Control or Ad-OSCAR (both 800 MOI) and were sacrificed a week later ($n = 10$ mice per each group) (**c**). Cartilage sections from their knee joints were subjected to immunohistochemistry for OSCAR (**d**) and Safranin-O/hematoxylin staining (**e**). Representative images are shown. The latter slides were used to score the following OA variables (**f**): The ratio of hyaline cartilage (HC) to calcified cartilage (CC) and synovitis ($n = 10$ mice per group). Scale bar, 25 μm . **g–i** The knee joints of C57BL/6J mice were IA-injected with Ad-Control or Ad-OSCAR weekly for 8 weeks and, starting 1 week after the first adenovirus injection, 0.5, 1, or 2 mg/kg

5-ASA or vehicle (Veh; PBS) was IA-injected weekly for 8 weeks starting 1 week after the first adenovirus injection. The last 5-ASA/vehicle injections occurred 1 week after the last adenovirus injection and 1 week before the sacrifice at week 9 ($n = 10$ mice per group) (**g**). Safranin-O/hematoxylin staining of cartilage sections (**h**) was then conducted. Representative images are shown. The slides were used to score the following OA variables (**i**): articular cartilage destruction (as indicated by the OARSI grade), osteophyte maturity, subchondral bone plate thickness (SBP Th.), and synovitis. The OARSI grade, synovitis, and osteophyte maturity data are shown as means \pm 95% confidence intervals (CI). Differences between groups were determined with the Kruskal–Wallis test followed by the Mann–Whitney U test. The HC/CC ratio and SBP thickness data were shown as means \pm s.e.m. Differences between groups were determined with a two-tailed t -test. Exact P values can be found in the accompanying Source Data. Scale bars, 25 μm .

5-ASA treatment attenuates OSCAR-related cartilage destruction in mice

Since (i) cartilage expresses more OSCAR in OA^{14,15}, (ii) collagen-II is the activating ligand of OSCAR¹⁰, and (iii) 5-ASA antagonizes OSCAR binding to collagen-II, we asked whether IA-injection of 5-ASA could attenuate the OA-like cartilage destruction induced by 8 IA Ad-OSCAR injections. Indeed, when the mice were co-injected weekly with 0.5, 1, or 2 mg/kg 5-ASA starting 1 week after the first Ad-OSCAR injection and sacrificed 1 week after the last 5-ASA injection (Fig. 1g), we found that 5-ASA reduced articular cartilage erosion (i.e., OARSI scores) as well as decreasing osteophyte development, SBP thickening, and synovitis (Fig. 1h, i). Moreover, as we will detail later, we found that the cartilage destruction induced by DMM surgery, which correlates with cartilage expression of OSCAR (see Fig. 7), was greatly ameliorated by IA injections of 5-ASA (see Figs. 6 and 7). Thus, 5-ASA may antagonize the ability of OSCAR to induce cartilage destruction.

It should be noted that mice treated weekly with IA 5-ASA injections for 3 or 8 weeks were viable, normally sized, had normal life-spans, and lacked gross morphological or histological abnormalities.

5-ASA powerfully targets PPAR γ and the eicosanoid pathway

Supplementary Fig. 3 and Fig. 1 together suggest that by binding to OSCAR, 5-ASA alters OSCAR signaling in chondrocytes, which both reduces chondrocyte OSCAR expression and associates with cartilage protection. To identify the 5-ASA targets in this signaling pathway, we conducted RNA-sequencing analysis on Ad-OSCAR-infected chondrocytes cultured on COL^{pep} with or without 5-ASA.

Compared to Ad-Control-infected chondrocytes, OSCAR overexpression resulted in 1515 DEGs, of which 682 were upregulated and 833 were downregulated. By contrast, compared to Ad-Control-infected chondrocytes, 5-ASA-treated OSCAR-overexpressing chondrocytes had 456 DEGs, of which 184 were upregulated and 272 were downregulated. Importantly, 5-ASA downregulated 82 of the 682 DEGs (12%) that were upregulated by OSCAR overexpression and upregulated 118 of the 833 DEGs (14%) that were downregulated by OSCAR overexpression. These DEGs were termed Flip-DEGs because 5-ASA reversed (flipped) the effect of OSCAR overexpression (Supplementary Data 2). Since Ad-OSCAR overexpression in murine knees induced cartilage destruction and OA-like disease and 5-ASA repressed that, we, therefore, designated the DEGs that were upregulated by OSCAR overexpression but then downregulated by 5-ASA as Flip^{catabolic}-DEGs because these genes could potentially promote cartilage destruction/OA: indeed, these DEGs included MMPs and ADAMTSs. Similarly, the DEGs that were downregulated by OSCAR overexpression but then upregulated by 5-ASA were designated Flip^{anabolic}-DEGs because these genes could potentially inhibit cartilage destruction/OA: indeed, these DEGs included collagen-II, ACAN, and the cartilage-anabolism marker SOX9 (Fig. 2a, b; Supplementary Data 2).

Moreover, pathway analysis showed that known cartilage catabolism and anabolism pathways in OSCAR-overexpressing chondrocytes were altered by 5-ASA treatment. Specifically, the Flip^{catabolic}

pathways included the inflammation and eicosanoid-related pathways (Fig. 2c). In particular, the Flip^{catabolic} genes in the eicosanoid-related pathway included prostaglandin-endoperoxide synthase 2 (*Ptgs2*, which encodes cyclooxygenase [COX]-2), arachidonate 5-lipoxygenase (*Alox5*, which encodes LOX-5), and their downstream genes (e.g., *Ptges*, *Alox5ap*, *Ltc4s*, *Ltb4r1*, and *Ltb4r2*) (Supplementary Fig. 4a). Moreover, the Flip^{anabolic} pathways included those that relate to collagen, NMDA-receptor and gap-junction trafficking, cholesterol-metabolism, and folate/amino-acid metabolism (Fig. 2d). Several of the latter are known to relate to cartilage-regeneration processes, including collagen production²² and glycine/serine metabolism, which is required for the biosynthesis of ECM collagen and glycoprotein²³. These transcriptomic changes, together with the in vitro chondrocyte, induced docking, and Ad-OSCAR-injection data, support the notion that 5-ASA may exert chondroprotective effects by altering the COL^{pep}-stimulated signaling of OSCAR on chondrocytes.

To assess the changes further, we identified the 14 transcription factors (TFs) whose expression was most strongly altered by 5-ASA treatment (Fig. 2e) and then conducted network analysis (Fig. 2f). This suggested that PPAR γ -encoded PPARG may play an important role in the effect of 5-ASA on chondrocytes. It was downregulated by OSCAR overexpression but this was flipped by 5-ASA. This is consistent with studies showing that 5-ASA upregulates PPAR γ in epithelial cells²⁴. Other important TFs may be EP300, which is a co-activator of PPAR γ ²⁵; SOX9, which is a cartilage-anabolism marker in OA²⁶; SREBF1, which mediates cholesterol metabolism²⁷, which is one of the 5-ASA-regulated pathways (Fig. 2); ATF4, which promotes SREBF1 by inhibiting its degradation²⁸ and may upregulate collagen synthesis²⁹ and amino-acid metabolism³⁰; and RXRA, which heterodimerizes with PPAR γ and may thereby regulate lipid/cholesterol metabolism³¹.

To further determine which FlipDEGs and FlipTFs could be particularly important 5-ASA targets in OA, we asked whether the 5-ASA-altered DEGs demonstrated similar expression patterns in response to other known drugs/compounds. For this, we conducted in silico analysis with Connectivity Map (CMap), a large dataset comprising the transcriptomes of >20 K drugs/compounds that have been used extensively for drug repurposing and mode-of-action analyses³². This analysis indicated how closely the 5-ASA-induced Flip-DEG profile resembled the DEG profiles induced by each of the >20 K drugs/compounds. We then took the top 10% of the most similar CMap profiles and listed the most enriched targets (see Methods for details). This revealed eight putative 5-ASA targets. Three have already been noted in the analyses above, namely, PTGS2/COX-2, RXRA, and PPARG. The other five predicted targets were ERBB2, TBXAS1, NRII2, PPARD, and RARG (Fig. 2g): these were also in the Flip^{catabolic} and Flip^{anabolic} gene sets (Supplementary Data 2), and two (PPARD and RARG) were in the 14 TFs that we found were most strongly altered by 5-ASA treatment (Fig. 2e). Moreover, Zhu et al.³³ showed that an RXR agonist can suppress OA and that this relies on activation of PPAR γ . In addition, like PTGS2/COX-2, TBXAS1 is also a key enzyme in the eicosanoid pathway (Supplementary Fig. 4a, b).

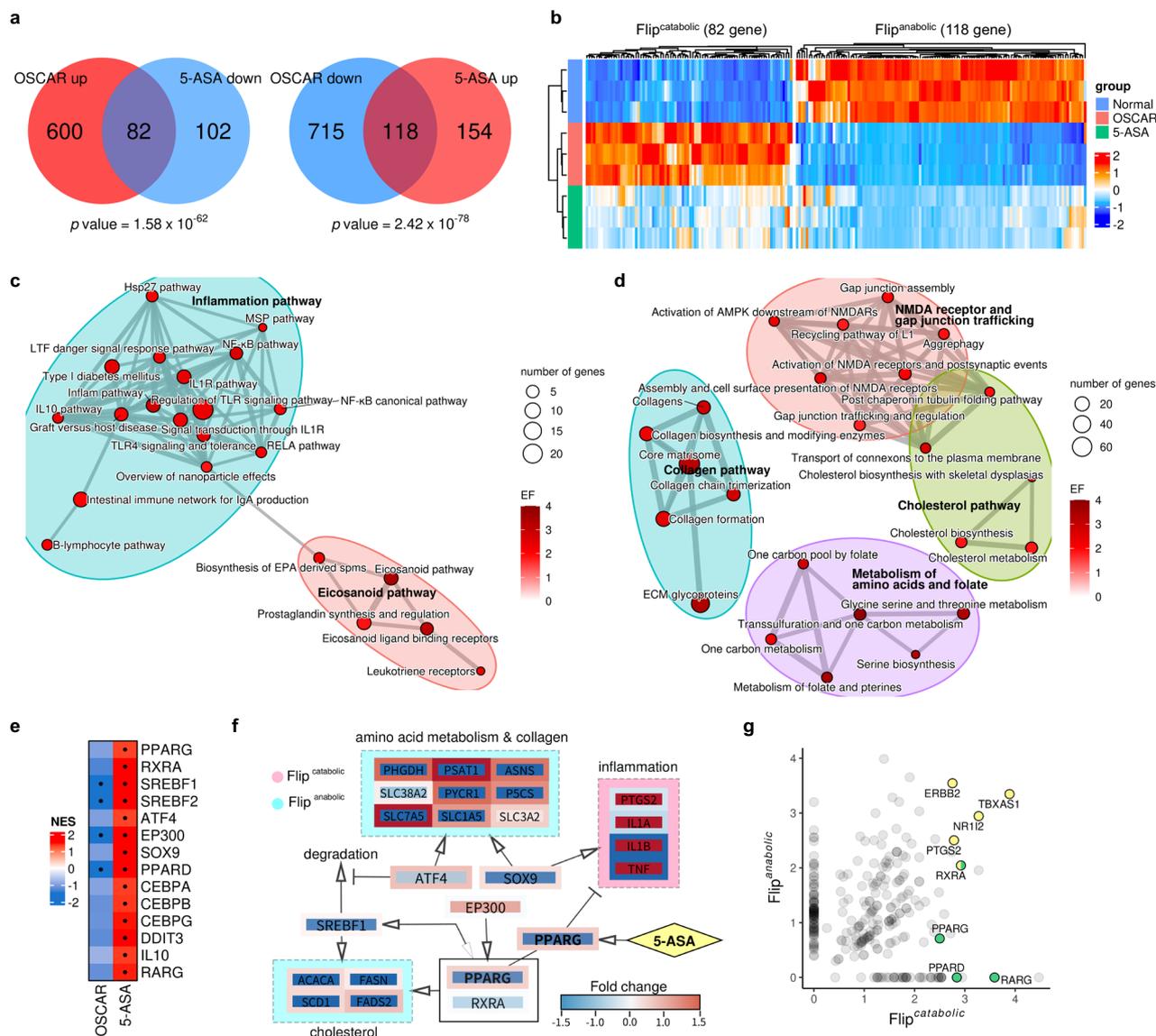


Fig. 2 | 5-ASA ameliorates OA by regulating the transcriptomic changes induced by OSCAR. **a** Identification of DEGs in Ad-OSCAR-infected chondrocytes relative to Ad-Control-infected chondrocytes and the effect of 5-ASA treatment on these DEGs. Chondrocytes infected with Ad-OSCAR were treated with or without 10 μ M 5-ASA. Chondrocytes infected with Ad-Control were not treated with 5-ASA. The total RNAs were subjected to RNA-seq analysis. The 82 genes that were upregulated by OSCAR overexpression but then downregulated by 5-ASA are denoted as Flip^{Up-Down} DEGs. The 118 genes that were downregulated by OSCAR overexpression but then upregulated by 5-ASA were designated Flip^{Down-Up} DEGs. **b** Heatmap of the Flip^{Up-Down} and Flip^{Down-Up} genes. **c, d** Network of the pathways that are inversely regulated ('Flip') by OSCAR and 5-ASA. The pathways are connected by significantly overlapping genes. Flip^{catabolic} pathways are shown (**c**) and Flip^{anabolic} pathways (**d**). Pathways are grouped with K-means clustering.

e Identification of the TF genes that operate downstream of the 'Flip' pathways (FlipTFs) in OSCAR-overexpressed and 5-ASA-treated chondrocytes. The normalized enrichment score (NES) for these TFs is shown. **f** Inferred regulatory network between the FlipTFs and the Flip pathway genes. Genes are colored according to fold change of OSCAR (center) and 5-ASA (border). The networks were visualized by Cytoscape v.3.8 software. **g** Identification of the 5-ASA-associated FlipDEGs and FlipTFs that are also strongly regulated by other FDA-approved drugs. The CMap database was searched for drugs that strongly altered the Flip^{catabolic} and Flip^{anabolic} DEGs in the same direction as 5-ASA. The Flip^{Up-Down} and Flip^{Down-Up} genes/TFs were then graphed on the x- and y-axis, respectively. The FlipDEGs (yellow) and FlipTFs listed in **e** (green) that are significantly enriched drug targets are highlighted. A hypergeometric test was used to conduct an enrichment analysis, assessing the extent of overlap between the two groups across the common gene space (**a**).

PPAR γ signaling in chondrocytes may mediate the cartilage-protective effects of 5-ASA

Of the DEGs/TFs that we identified, *Ptgs2*/COX-2, *Alox5*/LOX-5, and *Pparg*/PPAR γ were most strongly regulated by OSCAR overexpression in chondrocytes, and these effects were vigorously reversed by 5-ASA. Thus, by downregulating PPAR γ , OSCAR may upregulate COX-2 and LOX-5. These then promote inflammation because they are key arachidonic-acid metabolizers and convert it into inflammatory eicosanoids, namely, the prostaglandins (PGs), thromboxanes, leukotrienes (LTs), and lipoxins^{34,35}. COX exists as COX-1 and COX-2

isoforms. The latter produces PGE₂, which drives smooth muscle contraction, pain, fever, and vasodilation. Notably, specific COX-2 inhibitors have been used to treat OA and rheumatoid arthritis (RA) with a low risk of adverse gastrointestinal effects³⁶. Of the six LOX genes, LOX-5 produces LT³⁷, which activates leukocytes. Notably, LTB₄ plays an essential role in RA-associated pain and bone damage³⁸.

Since elucidating the molecular mechanisms by which 5-ASA protects cartilage could reveal therapeutic targets, we focused further on COX-2 and LOX-5 as either markers of the eicosanoid pathway or true targets. In either case, exploring the link between OSCAR, PPAR γ ,

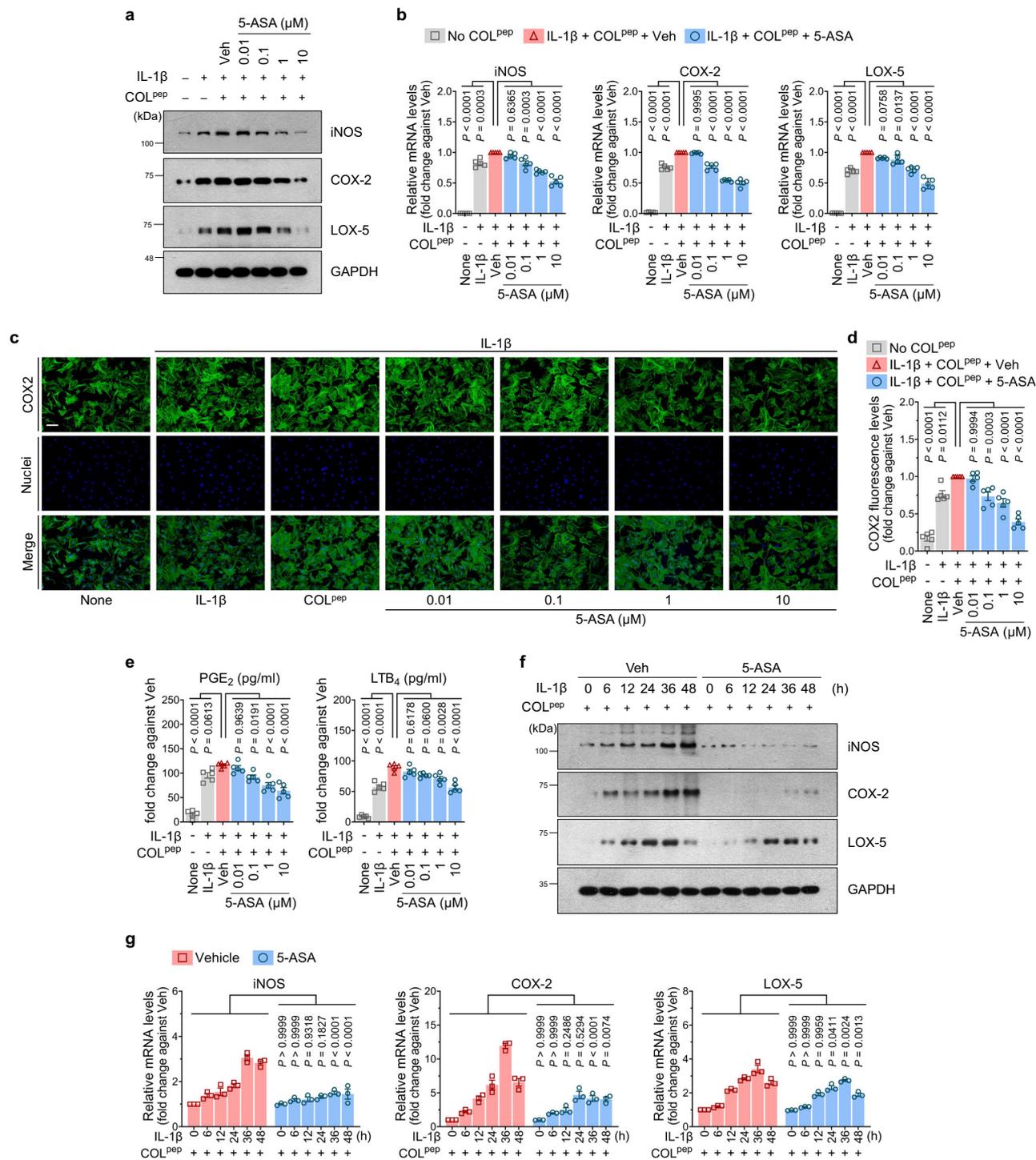


Fig. 3 | 5-ASA inhibits the PPARγ-COX-2 pathway in primary chondrocytes.

a–e Ad-OSCAR-infected mouse chondrocytes were cultured for 48 h on dishes that were coated with 2 μg/ml COL^{pep} or the GPIIb/IIIa control peptide together with 10 ng/ml IL-1β and either vehicle or the indicated concentration of 5-ASA (n = 5 independent primary chondrocyte cultures). **a** Western blotting with anti-iNOS, -COX-2, and -LOX-5 antibodies. **b** qRT-PCR analysis of iNOS, COX-2, and LOX-5 mRNA. **c, d** Immunofluorescence staining of COX-2. **c** COX-2 was stained green (upper boxes), while the nuclei were blue due to DAPI staining (middle boxes). The merged images are shown in the lower boxes. (Scale bar, 50 μm). **d** Quantification

of the fluorescence intensity in each group. **e** ELISA analysis of PGE₂ and LTB₄ concentrations released into the supernatant. **f, g** Primary mouse chondrocytes were cultured with 10 ng/ml IL-1β and COL^{pep} and iNOS, COX-2, and LOX-5 immunoblotting (**f**) and qRT-PCR (**g**) were performed (n = 5 independent primary chondrocyte cultures). The data are shown as means ± s.e.m. P-values were determined by one-way ANOVA followed by Tukey's multiple comparisons test (**b, d, e**) or two-way ANOVA followed by Sidak's post hoc test (**g**). Source data are provided as Source Data files.

COX-2, and LOX-5 could help illuminate the key role of PPAR γ in OA pathogenesis. Thus, we asked whether OSCAR binding to collagen-II affected the eicosanoid pathway in chondrocytes. Indeed, IL-1 β +COL^{pep}-treated Ad-OSCAR-infected chondrocytes demonstrated *Ptgs2*/COX-2 and LOX-5 protein/mRNA upregulation. Inducible nitric oxide synthase (iNOS), which produces the key inflammatory mediator nitric oxide³⁹, was also upregulated. Significantly, 5-ASA treatment inhibited all these effects (Fig. 3a, b). Immunofluorescence staining confirmed that IL-1 β +COL^{pep} upregulated *Ptgs2*/COX-2, and 5-ASA suppressed this effect (Fig. 3c, d). As expected, these changes also affected chondrocyte PGE2 and LTB4 expression: IL-1 β +COL^{pep} elevated the secretion of both mediators into the supernatant, and 5-ASA suppressed this (Fig. 3e). We then confirmed that 5-ASA downregulated *Ptgs2*/COX-2 expression via OSCAR by infecting chondrocytes with Ad-*Ptgs2* and then treating them with IL-1 β +COL^{pep} with or without 5-ASA: 5-ASA significantly reduced the overexpression of *Ptgs2*/COX-2. This was not observed when IL-1 β +COL^{pep} was not present, which indicates that 5-ASA suppressed *Ptgs2*/COX-2 expression via OSCAR (Supplementary Fig. 5a, b). The gain-of-function experiments conducted with COX2 via Ad-*Ptgs2* revealed that the overactivation of the eicosanoid pathway results in an opposing effect when compared to the impact of 5-ASA. The overexpression of *Ptgs2* exhibited a contrasting effect to that of 5-ASA concerning the expression of Flip^{catabolic} DEGs, including well-known markers of cartilage catabolism, such as *Mmp3*, *Mmp9*, *Mmp13*, and *Adamts5* mRNA, in chondrocytes (Supplementary Fig. 5c). The possibility that 5-ASA blocked COL^{pep}-induced OSCAR-mediated PGE2 production via *Ptgs2*/COX-2 was confirmed by infecting chondrocytes with Ad-sh*Ptgs2*, which silences *Ptgs2*/COX-2: when these cells were stimulated with COL^{pep}, they were unable to produce PGE2, as expected, and 5-ASA treatment had no effect on this (Supplementary Fig. 5d, e). IL-1 β +COL^{pep} treatment of primary (uninfected) chondrocytes also elevated COX-2, LOX-5, and iNOS protein/transcripts, and these effects were reversed by 5-ASA (Fig. 3f, g).

Since PPAR γ can inhibit COX-2 expression⁴⁰ and *Ptgs2*/COX-2 expression was strongly suppressed by 5-ASA, we speculated that COL^{pep}-stimulated OSCAR promotes *Ptgs2*/COX-2 by downregulating PPAR γ and that 5-ASA relieves this suppressive effect by competing with COL^{pep}. To test this, IL-1 β +COL^{pep}-treated primary chondrocytes were incubated with either 5-ASA or the PPAR γ -agonist rosiglitazone⁴¹, and PPAR γ expression was measured. As expected, IL-1 β +COL^{pep} downregulate PPAR γ expression. However, 5-ASA greatly increased it, in fact, even better than rosiglitazone (Fig. 4a). Thus, 5-ASA binding to OSCAR strongly induced PPAR γ . Next, we induced chondrocytes to overexpress PPAR γ with Ad-*Pparg* (Fig. 4b), cultured them with IL-1 β +COL^{pep} to upregulate OSCAR expression, treated them with 5-ASA, and measured *Ptgs2*/COX-2 expression. While IL-1 β +COL^{pep} increased *Ptgs2*/COX-2 expression as expected, overexpressing PPAR γ halved that effect, and this was further augmented when 5-ASA was also present (Fig. 4c). Moreover, overexpressing *Pparg* had the same effect as 5-ASA in terms of the Flip^{anabolic} DEGs (and known markers of cartilage anabolism^{7,8}) *Rxra*, *Col2a1*, *Acan*, and *Sox9* mRNA expression by the IL-1 β +COL^{pep}-treated chondrocytes: both treatments increased these mRNA levels (Supplementary Fig. 5f). These results together suggest that (i) when OSCAR expression in chondrocytes is increased by collagen binding, PPAR γ is downregulated, which upregulates *Ptgs2*/COX-2 expression and thereby elevates PGE2 secretion and inflammation; and (ii) 5-ASA treatment reverses this pro-inflammatory effect on the PPAR γ -COX-2-PGE2 axis.

5-ASA stimulates MSC chondrogenesis

The key role of PPAR γ in the mode-of-action of 5-ASA in chondrocytes suggested another possibility by which 5-ASA improves OA, namely, it may promote cartilage regeneration. This notion reflects the fact that (i) MSCs from OA patients differentiate into chondrocytes in vitro less

well than normal-donor MSCs⁴², and (ii) PPAR γ promotes human-MSC chondrogenesis in vitro⁴³. To test whether 5-ASA promotes chondrogenesis by blocking OSCAR activity, we first asked whether OSCAR could impair MSC chondrogenesis. Thus, the damaged/undamaged articular cartilage areas of ten OA patients who underwent total knee-replacement surgery (Supplementary Data 3) were identified with Alcian-Blue staining (which recognizes cartilage glycosaminoglycans). The damaged/undamaged areas were then subjected to OSCAR and PPAR γ immunohistochemistry. Significantly, OSCAR protein was very low in the undamaged cartilage but highly upregulated in the damaged cartilage, whereas PPAR γ protein demonstrated the opposite pattern (Fig. 4d). Thus, high OSCAR and low PPAR γ expression could potentially be associated with poor cartilage regeneration and MSC activity.

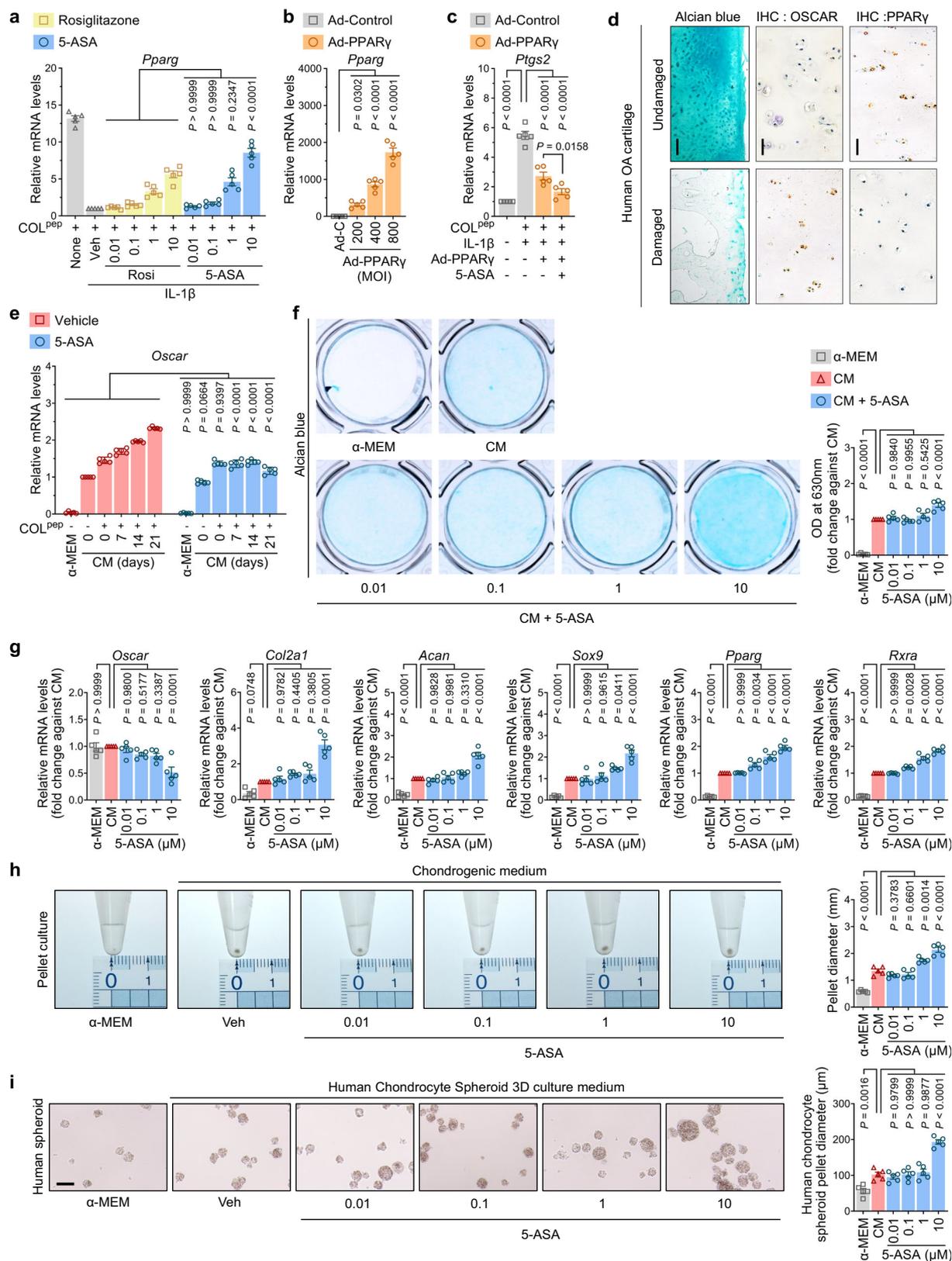
Next, we asked whether 5-ASA treatment promoted murine bone marrow-derived MSC differentiation into glycosaminoglycan-producing chondrocytes. We noted that after 21 days of culture in a chondrogenic medium containing COL^{pep}, the differentiating chondrocytes started to express OSCAR. This was suppressed when 5-ASA was also present (Fig. 4e). Notably, 5-ASA also increased chondrogenesis in a dose-dependent manner, as shown by greater Alcian-Blue staining (Fig. 4f). Moreover, this not only associated with decreased *Oscar* transcription, it also associated with increased expression of *Pparg*, the Flip^{anabolic} DEG *Rxra*, and the three markers cartilage-anabolism genes collagen-II/*Col2a1*, *Acan*, and *Sox9*²⁶ (Fig. 4g). The expression of the latter indicates that chondrocytes emerging in the presence of 5-ASA are capable of cartilage anabolism. Interestingly, if the bone marrow-derived MSCs were infected with Ad-sh*Pparg* before culture in chondrogenic medium containing COL^{pep}, 5-ASA could no longer increase cell expression of *Col2a1*, *Acan*, and *Sox9* (Supplementary Fig. 5g). This suggests that (i) PPAR γ can induce beneficial cartilage anabolism (as well as antagonize harmful eicosanoid pathway-mediated joint inflammation), and (ii) 5-ASA can promote the production of cartilage-anabolic chondrocytes in a PPAR γ -dependent manner.

The pro-chondrogenic effect of 5-ASA was also observed when human chondrocytes underwent pellet or 3-dimensional culture with soluble COL^{pep} with/without 5-ASA: 5-ASA clearly associated with greater pellet diameters (Fig. 4h), chondrocyte cohesion, and healthy growth (Fig. 4i). Thus, OSCAR expression associated with cartilage damage and suppressed PPAR γ expression, while 5-ASA promoted MSC chondrogenesis in a manner that relied on increased PPAR γ expression. This suggests that 5-ASA could potentially promote cartilage regeneration.

5-ASA may prevent cartilage destruction by blocking OSCAR-mediated upregulation of ECM degradation

OA chondrocytes demonstrate upregulation of the ECM-degrading enzymes MMP3, MMP9, MMP13, and ADAMTSS^{4,5}, which are crucial effectors of the cartilage destruction in OA⁴⁴, and downregulation of the ECM molecules collagen-II and ACAN⁴⁵. These changes are thought to be caused by the pro-inflammatory molecule IL-1 β ^{4,5}. Notably, our RNA-seq analysis showed that OSCAR overexpression strongly upregulated MMP3, MMP9, MMP13, and ADAMTSS, and downregulated collagen-II, ACAN, and the cartilage-anabolism marker SOX9, and this was powerfully reversed by 5-ASA treatment. This was confirmed by immunoblotting and RT-PCR of primary chondrocytes treated with IL-1 β +COL^{pep} or IL-1 β alone (Supplementary Fig. 6).

Notably, when IL-1 β -stimulated chondrocytes were treated with 5-ASA for up to 30 min, we observed that it had no effect on the strong but transient IL-1 β -induced increase in MAPK and NF- κ B signaling (Supplementary Fig. 7a, b). This suggests that 5-ASA ameliorates OA by reversing the longer-term OSCAR-associated pro-inflammatory signaling generated by IL-1 β rather than by modulating other signaling pathways in OA. Thus, OSCAR may promote cartilage catabolism and inhibit cartilage anabolism, and 5-ASA may reverse this.



5-ASA treatment attenuates DMM surgery-induced OA, even when administered well after disease onset

We next asked whether IA injection of 0.5, 1, or 2 mg/kg 5-ASA attenuated DMM surgery-induced OA in mice. Thus, 5-ASA was injected for 8 weeks starting 1 week after surgery and the mice were sacrificed at 9 weeks (Fig. 5a). 5-ASA strongly inhibited articular-cartilage erosion

and other pathological signs in the affected knee in a dose-dependent fashion (Fig. 5b, c). This was confirmed by contrast agent-enhanced cartilage 3D micro-computed tomography: 5-ASA markedly inhibited SBP thickening and bone-volume increase (Fig. 5d, e). Thus, local 5-ASA administration significantly reduced trauma-induced articular-cartilage degeneration.

Fig. 4 | 5-ASA enhances PPAR γ signaling in chondrocytes and chondrogenesis. **a** Primary chondrocytes were treated without IL-1 β or with 10 ng/ml IL-1 β and 10 μ M 5-ASA or 10 μ M rosiglitazone (Rosi), and *Pparg* mRNA was measured with qRT-PCR. **b** Primary chondrocytes were infected with Ad-Control (Ad-C; 800 MOI) or the indicated Ad-PPAR γ MOI for 2 h, and *Pparg* mRNA was measured with qRT-PCR. **c** Primary chondrocytes were infected with 800 MOI Ad-PPAR γ and then treated with 10 ng/ml IL-1 β with or without 5 μ M 5-ASA. COX-2/*Ptgs2* mRNA was determined by qRT-PCR ($n = 5$ independent primary cultures in **a–c**). **d** Articular cartilage from ten patients obtained during total knee replacement surgery was subjected to Alcian-Blue staining (left) and IHC for OSCAR and PPAR γ expression (middle and right, respectively). The damaged and undamaged sections were assessed separately. Representative Alcian blue-stained (scale bar, 100 μ m) and IHC (scale bar, 50 μ m) images are shown. **e** Murine bone marrow-derived MSCs were cultured in a chondrogenic medium (CM) with or without 5-ASA for 7, 14, and 21 days, and qRT-

PCR was conducted to determine *Oscar*. **f–g** Bone marrow-derived MSCs were cultured in a chondrogenic medium with or without 5-ASA for 3 weeks, stained with Alcian Blue, and photographed (left, **f**). Alcian-Blue activity was quantified by measuring the absorbance at 630 nm (right, **g**). qRT-PCR was conducted to determine *Oscar*, *Col2a1*, *Acan*, *Pparg*, *Sox9*, and *Rxra* mRNA expression (**g**). **h** Bone marrow-derived MSCs were subjected to pellet culture in e-tubes for 3 weeks with or without 0.01, 0.1, 1, and 10 μ M 5-ASA, after which the pellet diameter was measured with a micro ruler ($n = 5$ independent primary cultures in **e–h**). **i** Human chondrocytes were subjected to spheroid culture in a 3D microenvironment with or without 0.01, 0.1, 1, and 10 μ M 5-ASA for 1 week, and the diameter of the spheroids was measured ($n = 5$ independent cultures in **i**). The data are shown as means \pm s.e.m. *P*-values were obtained by one-way ANOVA followed by Tukey's multiple comparisons test (**b, c, f–i**) or two-way ANOVA followed by Sidak's post hoc test (**a, e**). Exact *P*-values were provided in the Source Data file.

Next, to determine whether 5-ASA can reduce OA when given well after OA is evident, 5-ASA treatment was only started 5 weeks after DMM surgery (Fig. 5f). In the untreated group, severe cartilage erosion, accompanied by the development of osteophytes and thickening of the subchondral bone plate, along with notable synovitis, were observed. Conspicuously, the administration of 5-ASA during weeks 5–8 demonstrated a significant amelioration of these OA parameters (Fig. 5g, h). Notably, the 5-ASA-induced reduction in disease was as large as when 5-ASA was administered for the whole 8 weeks (Fig. 5b, c). The patterns were also observed for the other markers of OA (Fig. 5).

We then showed that 5-ASA could even induce DMM surgery-damaged cartilage to recover when it was first started after the disease had progressed to severe degenerative OA, namely, 8 weeks after DMM (Fig. 6a). Hence, mice subjected to a 4-week treatment with 5-ASA from weeks 8–11 exhibited a decrease in several OA markers when contrasted with mice at the 12-week post-DMM surgery stage. In fact, the final OARSI grade of the 5-ASA-treated mice sacrificed at week 12 was much lower than that of untreated mice that were sacrificed at week 8. This was also true for the other OA indicators. Significantly, the treated mice that were killed at week 12 had thicker cartilage than the mice that were sacrificed at week 8 (Fig. 6b, c). These findings suggest that 5-ASA could not just arrest OA progression; it could reverse it. However, additional studies are needed to confirm this.

5-ASA treatment in OA protects the cartilage from destruction and is associated with the downregulation of OSCAR and ECM-degrading enzymes

Immunohistochemistry of the knee cartilage of mice with DMM-induced post-traumatic OA showed that the surgery upregulated OSCAR protein expression, as expected^{14,15} and 5-ASA reversed this (Fig. 7a). Moreover, DMM surgery significantly upregulated MMP3, MMP13, and ADAMTS5 and downregulated COL2A1 and ACAN, and these effects were all markedly improved by 5-ASA treatment (Fig. 7). The latter findings are consistent with our RNA-seq, RT-PCR, and immunoblotting analyses.

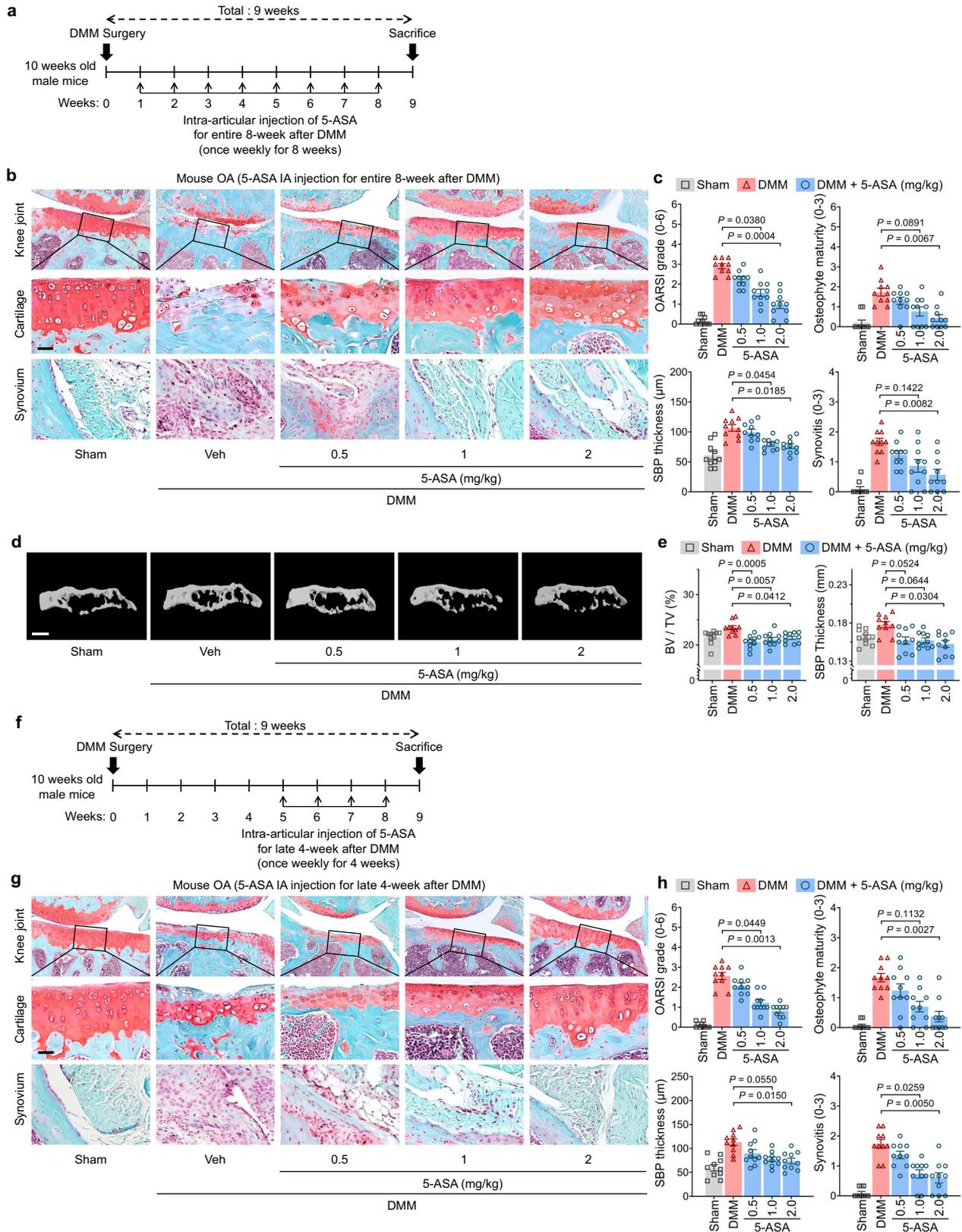
Discussion

The OA hallmark is the tipping of the fine balance between chondrocyte production of ECM and chondrocyte-mediated ECM catabolism: the latter predominates, which results in cartilage destruction. This reflects that enzymatic degradation, oxidative stress, and mechanical stress⁴⁶ lead to the production of ECM fragments (including COL^{pep}), which are recognized as damage-associated molecular patterns (DAMPs) by receptors on chondrocytes. The DAMP signals also induce proinflammatory cytokines that promote ECM catabolism and interrupt ECM anabolism. These factors together decrease chondrocyte numbers, which reduces their ability to maintain cartilage homeostasis⁴⁷.

OSCAR may play an important role in these osteoarthrogenic mechanisms because it recognizes the triple-helix collagen peptide^{10–12}. This notion was advanced by our previous study showing that OA cartilage in humans and mice expresses more OSCAR than normal cartilage^{14,15}. The present study further supported this hypothesis since we found that simply overexpressing OSCAR in articular joints led to OA-like cartilage destruction and inflammation. Moreover, downregulating OSCAR expression by IA-injection of shOSCAR-expressing adenovirus significantly ameliorated DMM-induced OA (Supplementary Fig. 1). Thus, OSCAR may play a very important role in OA pathogenesis.

The putative key role of OSCAR in OA, in turn, suggests that OSCAR antagonists of OSCAR-collagen binding could suppress OA-associated articular cartilage destruction in humans. Here, we report our discovery that 5-ASA can serve as an OSCAR antagonist that effectively reduces DMM-induced OA and the cartilage destruction generated by OSCAR overexpression in the joint. It should be noted that during the writing of this paper, Li et al.⁴⁸ reported that culturing human osteochondral explant models of OA with 5-ASA downregulated cartilage degradation. While they did not link this effect to OSCAR or conduct in vivo experimentation, these findings are highly consistent with our own, which together suggest that 5-ASA may have marked chondroprotective effects.

5-ASA is an anti-inflammatory drug that is widely used to treat IBDs, especially UC⁴⁹. Here we show that it may also be suitable as a DMOAD since it not only halted cartilage destruction in an animal model of OA, it also appeared to induce cartilage regeneration: even when 5-ASA was first administered in late-stage (8–11-week) murine OA, when there is immense cartilage damage, the OARSI grades recovered markedly and the cartilage thickness was greater than that of untreated mice that were sacrificed at week 8. Our mechanistic analyses suggest that these therapeutic properties are due to the ability of 5-ASA to bind to OSCAR, thereby triggering OSCAR-PPAR γ signaling that simultaneously (i) antagonizes inflammation and (ii) promotes chondrogenesis. With regard to the former, we found that 5-ASA competed with collagen for binding to OSCAR, and its binding to OSCAR upregulated PPAR γ . This downregulated the eicosanoid pathway, including COX-2 and its generation of PGE2 (Supplementary Fig. 8). The human osteochondral explant study of Li et al.⁴⁸ also observed that culture of the explants with 5-ASA downregulated COX-2. It should be noted that while it is widely believed that systemic administration of COX-2 inhibitors (i.e., common nonsteroidal anti-inflammatory drugs) does not associate with chondroprotective effects in OA, a recent systematic review suggested that some COX-2 inhibitors could act as DMOADs if they are injected IA⁵⁰. Moreover, another recent systematic review found that even when injected systemically, some COX-2 inhibitors (e.g., celecoxib) can modify the cartilage, bone, and synovial disease in OA, and these effects are mediated by the regulation of prostaglandins and direct changes to the tissues⁵¹. Since our 5-ASA treatment in mice involves IA injections and is



potentially a novel drug for OA, it is thus possible that COX-2 and LOX-5 could be effectors of OA. Alternatively, they are simply markers of the eicosanoid pathway. With regard to the potential role of OSCAR-PPAR γ signaling in chondrogenesis, we showed that 5-ASA may also improve OA by enhancing MSC chondrogenesis, chondrocyte aggregation and growth, and cartilage repair, which is a highly desirable attribute as a

DMOAD. It is likely that PPAR γ also participates in this regenerative outcome since it was upregulated by 5-ASA during chondrogenesis in vitro, and both 5-ASA treatment and overexpressing PPAR γ caused the developing chondrocytes to gain cartilage anabolic properties.

The importance of the OSCAR-PPAR γ signaling in OA is supported by the known roles of PPAR γ , which is a ligand-activated TF

Fig. 5 | 5-ASA attenuates post-traumatic OA. **a–c** C57BL/6J mice were subjected to sham operation or DMM surgery and then IA-injected once per week for the 8-week observation period with vehicle (Veh) or 5-ASA (0.5, 1, or 2 mg/kg) and sacrificed 9 weeks after the operation ($n = 10$ mice per each group) (**a**). **b** Representative Safranin-O staining and fast green counter staining images. Scale bar, 25 μm . **c** Quantitation of the following OA variables: OARSI grade, osteophyte maturity, subchondral bone plate thickness, and synovitis. **d, e** Representative reconstructed micro-CT images and quantitative analysis of mouse SBPs 10 weeks after DMM surgery compared to sham controls (**d**). Scale bars, 1000 μm .

e Quantitation of the SBP variables, namely, SBP thickness and bone volume fraction (BV/TV). $n = 10$ mice per each group. **f–h** C57BL/6J mice were injected as described in (**a**), except the 5-ASA injections started at 5 weeks (**f**). Representative images are shown (**g**). OA variables were quantitated (**h**) as described in (**c**). The OARSI grade, synovitis, and osteophyte maturity data are shown as means \pm 95% confidence intervals (CI). Differences between groups were determined with the Kruskal–Wallis test followed by the Mann–Whitney U test. Means \pm s.e.m. with two-tailed t -test for SBP thickness. Exact P values can be found in the accompanying Source Data. Scale bars, 25 μm .

that plays key roles in inflammation, fibrosis, and tissue repair⁵². Moreover, PPAR γ agonists protect animal models from OA, and these effects are mediated by their anti-inflammatory properties in vitro and in vivo⁵². In addition, Zhu et al.³³ showed recently that a retinoic acid metabolism blocking agent can suppress DMM-induced inflammatory signaling and OA and that this depends on the activation of PPAR γ . However, the exact molecular mechanisms by which such PPAR γ agonists improve OA have not been determined. Vasheghani et al.⁵³ also showed that mice in which PPAR γ was inducibly knocked out developed very severe accelerated DMM surgery-induced OA. Thus, our study greatly advances our knowledge about the in vivo role of PPAR γ in articular cartilage homeostasis, as well as confirming that upregulating this molecule may be a viable therapeutic target for OA.

Our finding that 5-ASA protected joints from OA by promoting the anti-inflammatory properties of PPAR γ is consistent with UC research: multiple studies show that 5-ASA largely improves UC by increasing intestinal-wall expression of PPAR γ , which downregulates local cytokine and inflammatory-mediator production⁵⁴. The mode-of-action of 5-ASA in UC and OA exhibits similarities, which aligns with the observation that these two diseases share several pathogenic changes⁵⁵.

Thus, IA delivery of 5-ASA may have considerable therapeutic potential in OA. This also raises the possibility that systemic administration of 5-ASA that is not formulated for bowel selectivity could be useful for OA that involves multiple joints. The feasibility of 5-ASA as a DMOAD is further supported by the fact that it and its precursors (e.g., sulfasalazine, also known as azulfidine) or derivatives (e.g., 4-aminosalicylic acid, acetylsalicylic acid, methyl salicylate, and 4-aminobenzoic acid⁵⁶) are already being used for human therapy. For example, sulfasalazine is both the first 5-ASA to be widely used for IBD and an effective disease-modifying anti-rheumatic drug for RA⁵⁷. Moreover, oral and topical 5-ASA has undergone years of formulation development with large-scale clinical trials and is very safe⁵⁸.

In summary, our study shows that 5-ASA has chondroprotective effects that significantly ameliorate OA by modulating the OSCAR-PPAR γ axis. Studies with other OA models and humans are warranted. Notably, OSCAR is a highly complex and multifactorial mediator: our RNA-seq analyses showed that OSCAR also downregulates several other signaling pathways, and 5-ASA reverses this. Moreover, PPAR γ agonism can involve non-inflammatory pathways^{52,59}, and 5-ASA also modulates IBD by non-PPAR γ pathways⁶⁰. Thus, further research on the roles of these pathways in the protective effects of 5-ASA on articular cartilage is also needed. Research on the mechanisms by which OSCAR overexpression alone drives OA pathogenesis is also warranted.

Methods

Mice

Murine experiments were conducted with male 10–11-week-old C57BL/6J (C57BL/6BomTac, DBL, South Korea) or Institute of Cancer Research (ICR) mice (IcrTac; ICR, DBL, South Korea). All mice were housed in pathogen-free barrier facilities at 5 or less per cage at 24–26 $^{\circ}\text{C}$, humidity ranging from 30–60%, and with a 12 h light/dark cycle. The mice were randomly allocated to each experimental group. In accordance with the ethical guidelines for animal research, we

rigorously implemented animal welfare monitoring and euthanasia practices throughout the study. All animal experiments were approved by the Institutional Animal Care and Use Committees (IACUC, Protocol No: IACUC 18–109, 20–047, and 21–076) of Ewha Womans University and followed the National Research Council and ARRIVE Guidelines.

Human samples

Cartilage tissues with OARSI grade 6 and the surrounding normal cartilage were acquired during total knee replacement surgery from ten patients with OA. The patients were 63–78 years old, and three and seven were male and female, respectively (Supplementary Data 3). To rule out the effects of other underlying diseases, we ensured that none of the patients had RA, metabolic disease, or other inflammatory diseases at the time of surgery. The institutional review board of Yonsei University (Protocol No. IRB 3-2018-0251), Gangnam Severance Hospital, South Korea, approved the use of the articular cartilage. All participants provided written informed consent authorizing the utilization of their tissue samples for research purposes and the publication of information that could potentially identify individuals.

Recombinant adenoviruses and 5-ASA

Vector Biolabs (Malvern, PA, USA) manufactured the adenoviruses that expressed OSCAR (Ad-OSCAR; catalog No. ADV-267721), Ad-Control (1060), Ad-shControl (1122), shOSCAR (Ad-shOSCAR; shADV-267721), COX-2 (Ad-Ptgs2; ADV-281024), shCOX-2 (Ad-shPtgs2; shADV-281024), PPAR γ (Ad-PPAR γ ; ADV-269122), or shPPAR γ (Ad-shPparg; shADV-269122). 5-ASA was obtained from Sigma-Aldrich (Cat# A3537; St Louis, MO, USA) and dissolved in PBS.

Adenovirus-induced murine OA and treatment with 5-ASA

Experimental OA was induced in C57BL/6J WT by IA injection of Ad-OSCAR. Thus, the IA space of the right knee joint was injected along the patellar tendon with 1×10^9 plaque-forming units of Ad-OSCAR in phosphate-buffered saline (PBS; pH 7.4) (total volume, 10 μl) once a week. Mice injected with Ad-Control or the PBS vehicle served as controls. In one experiment, the weekly adenovirus injections were conducted 3 times and the mice were sacrificed a week later at week 3. In the second experiment, the adenovirus injections were conducted 8 times, and 8 weekly IA injections with 0.5, 1, or 2 mg/kg 5-ASA were also given starting 1 week after the first adenovirus injection. The mice were sacrificed at week 9.

DMM surgery-induced murine OA and treatment with Ad-shOSCAR or 5-ASA

DMM surgery-induced OA was induced in C57BL/6J WT male mice by surgically removing the medial meniscus ligament from the right knee joint of the hind limb^{18,19,61,62}. Male mice were selected for the experiments due to a higher occurrence of the posttraumatic osteoarthritis model in males compared to females in murine studies⁶³. Female hormones exhibit protective effects on cartilage, whereas male hormones exacerbate the condition⁶⁴. Sham-operated mice served as controls. The sham operation involved conducting the same surgery on the contralateral knee but without removing the medial meniscus ligament. The mice were sacrificed 9 weeks after surgery. In one

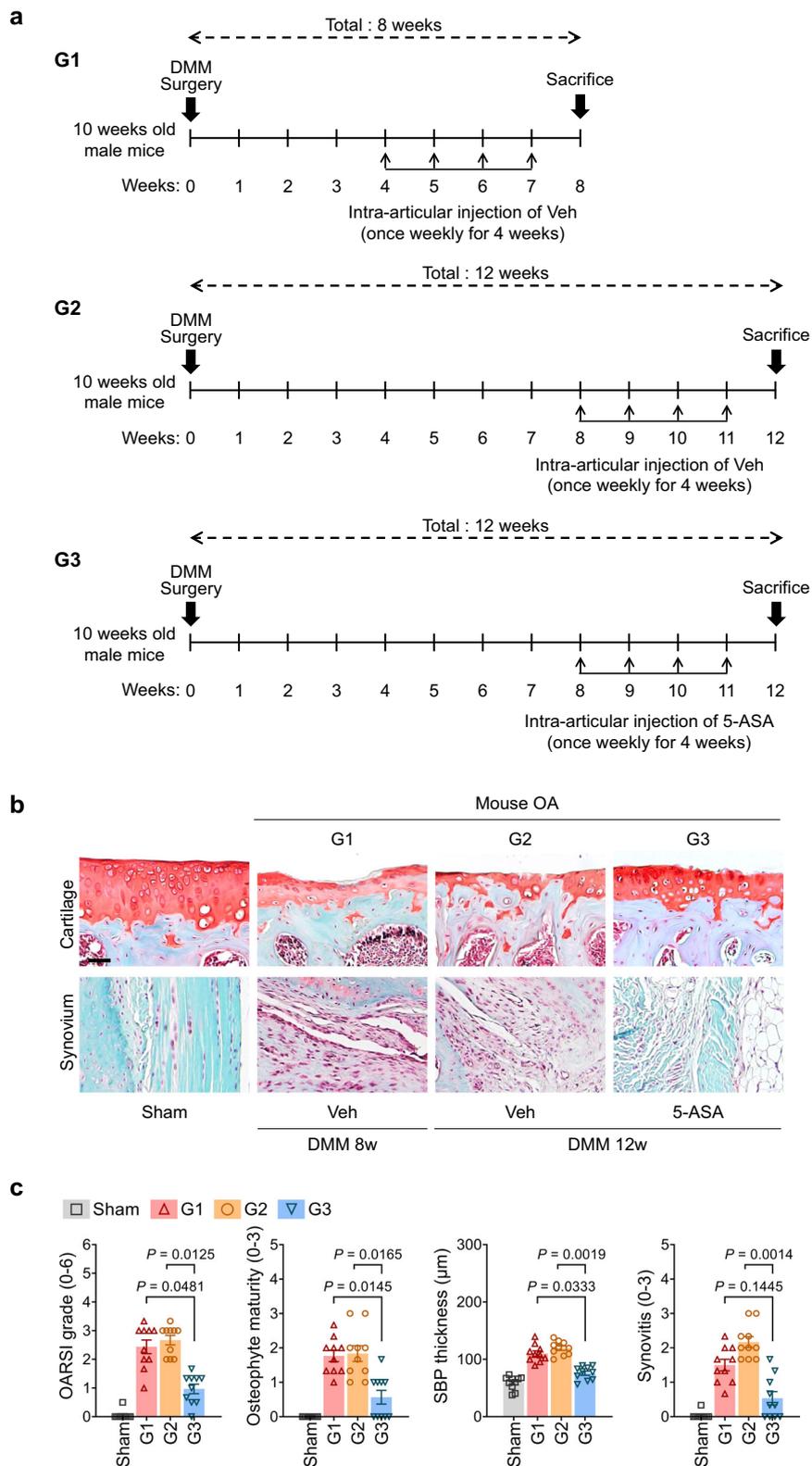


Fig. 6 | 5-ASA induces cartilage regeneration, even when administered in late-stage OA. a Mice were subjected to sham operation or DMM surgery and then IA-injected once per week for the indicated 4-week prior to sacrifice with vehicle (Veh; G1 and G2) or 5-ASA (2 mg/kg; G3) and sacrificed 9 (G1) or 12 weeks (G2 and G3) after the operation ($n = 10$ mice per group). **b** Representative Safranin-O staining and fast green counter staining images. Scale bar, 25 μm . **c** Quantitation of the following OA

variables: OARS grade, osteophyte maturity, subchondral bone plate thickness, and synovitis. The OARS grade, synovitis, and osteophyte maturity data are shown as means \pm 95% confidence intervals (CI). Differences between groups were determined with the Kruskal–Wallis test followed by the Mann–Whitney U test. Means \pm s.e.m. with two-tailed t -test for SBP thickness. Exact P values can be found in the accompanying Source Data. Scale bars, 25 μm .

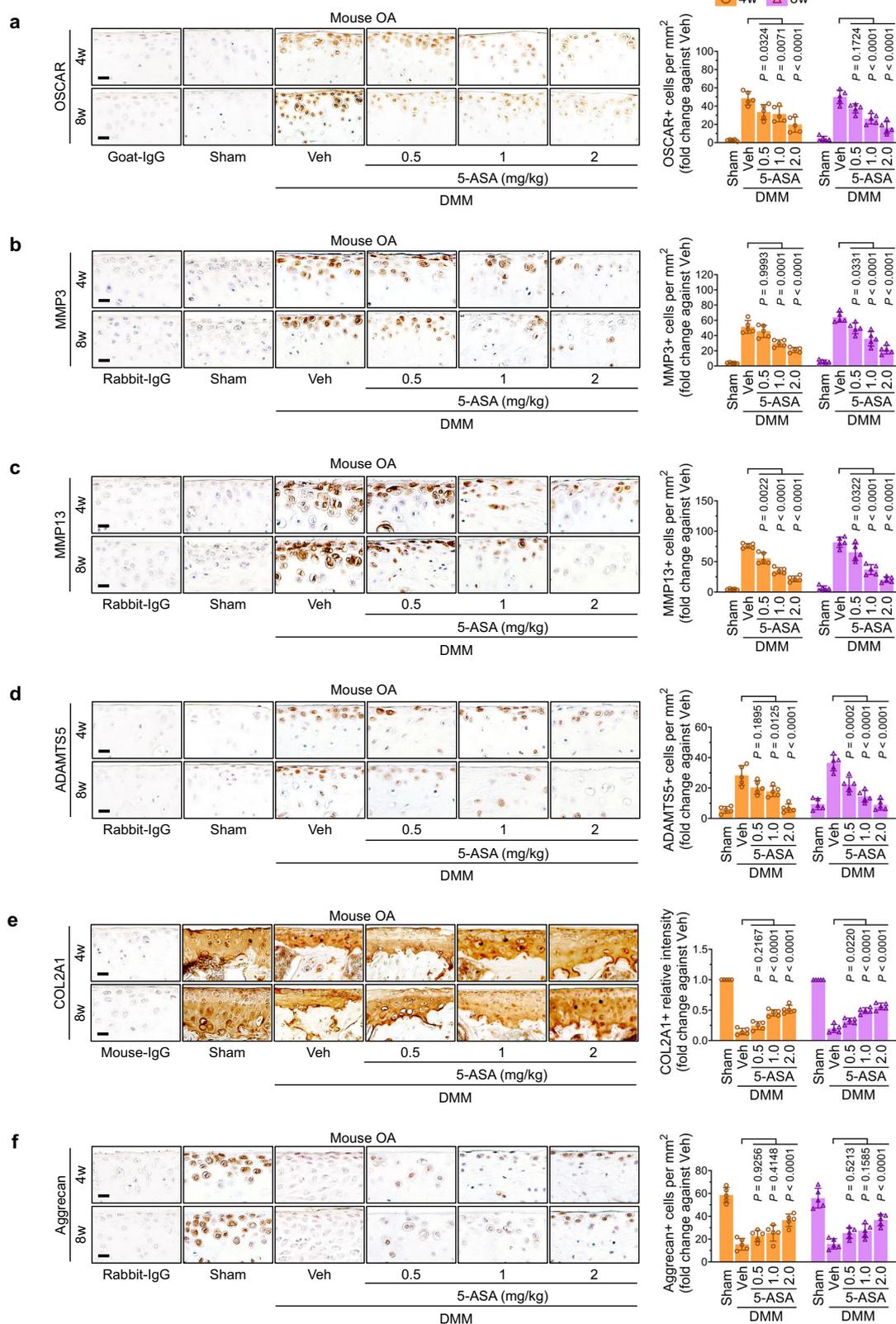


Fig. 7 | 5-ASA reduces catabolism and enhances anabolism in OA mouse joint tissues. **a–f** C57BL/6J mice were subjected to sham operation or DMM surgery, IA-injected with vehicle (Veh) or 5-ASA (0.5, 1, and 2 mg/kg) for 8 weeks as shown in Fig. 5a, and sacrificed 9 weeks after the operation ($n = 10$ mice per each group). The joint tissues were subjected to immunohistochemistry for OSCAR (**a**), MMP3 (**b**),

MMP13 (**c**), ADAMTS5 (**d**), ACAN (**e**), and COL2A1 (**f**) and the protein expression levels were quantified. Scale bar, 25 μm . The data are shown as mean \pm s.e.m. ($n = 5$ for each group; nonparametric test). P -values were obtained by two-way ANOVA was performed followed by Sidak's multiple comparisons test. Source data are provided as Source Data files.

experiment, OSCAR was knocked down with weekly IA injections of Ad-shOSCAR starting 1 week after DMM surgery and ending 1 week before sacrifice. In other experiments, the mice were IA injected with 0.5, 1, or 2 mg/kg 5-ASA or 2 mg/kg vehicle once weekly, either 8 times starting 1 week after surgery (i.e., treatment over the whole OA period) or 4 times starting 5 weeks after surgery (i.e., treatment for the last half of the OA period). In both regimens, the last 5-ASA injection occurred 1 week before sacrifice at week 9.

Articular chondrocyte isolation and adenovirus-mediated OSCAR overexpression

Murine articular chondrocytes were isolated from the femoral condyles and tibial plateaus of 4–5-day-old ICR or C57BL/6J WT mice by digestion with 0.2% collagenase type II. After culture for 48 h in Dulbecco's modified Eagle's medium (DMEM; HyClone, Logan, UT, USA) containing 10% fetal bovine serum (FBS), the cells were infected with the indicated MOIs of Ad-OSCAR or Ad-Control for 2 h and then cultured for an additional 24 h alone or with 5-ASA or pharmacological agents as described below. Normal human articular chondrocytes were isolated similarly from the normal healthy cartilage that was excised from a patient with OA who underwent total knee replacement surgery.

Histological analysis of OA

The knee joints of mice were fixed in 10% formaldehyde at 4 °C for >24 h, decalcified in 0.5 M ethylenediaminetetraacetic acid in PBS (pH 7.4) for 2 weeks, embedded in paraffin, sliced into 5- μ m sections, and stained with hematoxylin and eosin, 0.1% Safranin-O (s8884; Sigma-Aldrich, St Louis, MO, USA), and 0.05% Fast green FCF (f7258; Sigma-Aldrich, St Louis, MO, USA). Sclerosis and articular cartilage destruction were identified by safranin-O staining and measured with OsteoMeasureXP (OsteoMetrics, Inc., Atlanta, GA, USA), Image-pro plus (v4.5, Media Cybernetics, Inc., Rockville, USA), Adobe Photoshop (v9.0, San Jose, CA, USA), and an Olympus DP72 charge-coupled device camera (v2.1, Olympus Corporation, Tokyo, Japan). Articular cartilage destruction was scored by using OARSI grades (0–6), which is a standard OA-grading system^{18,62} (Supplementary Data 4). The OARSI grades of the medial tibia were assessed by averaging the scores of three experienced investigators. The ratio of hyaline cartilage to calcified cartilage, osteophyte maturity, and synovitis⁶⁵ were also determined (Supplementary Data 5). Moreover, subchondral bone sclerosis was determined by measuring the SBP thickness.

Generation of hOSCAR-Fc fusion protein and the Tyr166Ala, Tyr200Ala, and Ser166Ala mutants

293 F cells were transfected with a pVITRO1-Fc clone that expressed hOSCAR-Fc, namely, the extracellular domain (amino acids 19–233) of human OSCAR fused to the Fc region of human IgG1. The secreted purified protein was then loaded into a Thermo Scientific™ Pierce™ Protein G-Sepharose bead column (Thermo Fisher Scientific, Waltham, MA, USA) and eluted with elution buffer (100 mM glycine, pH 2.0, and 1 M Tris-Cl, pH 7.0; Duchefa Biochemie, 2003 RV Haarlem, the Netherlands) to immediately neutralize the protein. The tubes containing high concentrations of protein were collected, extensively dialyzed against PBS, and kept frozen at –80 °C. The Tyr166Ala, Tyr200Ala, and Ser166Ala mutants of hOSCAR-Fc were generated by a PCR-based method.

High-throughput screening of small compound libraries

In total, the libraries contained 3287 compounds. They consisted of 1316 natural compounds from Med Chem Express (MCE; Monmouth Junction, NJ, USA) and 1971 from the FDA-approved Drug library (ApexBio Technology; Houston, TX, USA). For primary screening, we established an ELISA-based high-throughput screening method using hOSCAR-Fc fusion protein and the OSCAR-binding triple-helical

collagen peptide (COL^{pep}) in the 96-well plate scale. COL^{pep} (short-form sequence: GPC-(GPP)₅-GPOGPAGFO-(GPP)₅-GPC-amide; alignment anchor residues are underlined) was from the University of Cambridge (CAS No. 2260906-29-2; Trinity Ln, CB2 1TN, UK). Its purity was confirmed by high-performance liquid chromatography. GPP10, which is a collagen-mimetic peptide (GPC-(GPP)₁₀-GPC-amide; CAS No. 2260816-94-0; University of Cambridge), served as a negative control peptide. Both were dissolved in 0.01 M acetic acid. Screening was initiated by pre-coating 96-well plates with 2 μ g/ml COL^{pep} overnight at 4 °C and pre-incubating each library compound at concentrations ranging from 0.0001 to 50 μ M for 1 h with 0.1 μ g/ml hOSCAR-Fc fusion protein. The hOSCAR-Fc mixtures were then added to the COL^{pep}-bearing plates for 1 h. Horseradish peroxidase-conjugated goat anti-human IgG (Cat# LF-SA8014H; Ab Frontier, 1:3000 dilution) served as the secondary antibody. The optical density at 450 nm (OD 450 nm) was then determined. All compounds were tested five times.

Verification testing of candidate molecules identified by screening

For verification, the COL^{pep}/hOSCAR-Fc-based ELISA described above was used with increasing concentrations of candidate molecules. Moreover, to determine whether the candidates could compete with collagen-II for binding to cell-surface OSCAR, murine chondrocytes were cultured for 48 h in plates on which 2 μ g/ml COL^{pep} had been immobilized, infected with Ad-OSCAR for 2 h, and then treated with each candidate molecule for 48 h. Alternatively, murine chondrocytes were not infected with Ad-OSCAR. OSCAR mRNA/protein was isolated and measured by qRT-PCR and Western blotting, respectively.

RNA isolation and qRT-PCR

Total RNAs from primary chondrocytes or bone marrow-derived MSCs were isolated by using TRIzol (Invitrogen, Carlsbad, CA, USA). Total RNAs from murine and human knee joint tissues were isolated by using the RNA Mini Kit (Life Technologies, Carlsbad, CA, USA). The RNAs were reverse-transcribed to generate complementary DNA (cDNA) by using the Superscript cDNA synthesis kit (Invitrogen) according to the manufacturer's instructions. qRT-PCR was performed using the KAPA SYBR Green fast qPCR kit (Kapa Biosystems, Inc., Wilmington, MA, USA) on a Step One Plus RT-PCR machine (Applied Biosystems, Foster City, CA, USA). The samples were tested in triplicate and the data were normalized by using β -actin as a housekeeping gene. Supplementary Data 6 provides the full list of primers.

Primary culture of articular chondrocytes with COL^{pep}, IL-1 β , 5-ASA, and/or rosiglitazone

The cultured chondrocytes were normal human or murine chondrocytes, or murine chondrocytes that were infected with Ad-OSCAR, Ad-Control, Ad-PPAR γ , or Ad-PTGS2 at the indicated MOIs for 2 h. The chondrocytes were cultured in DMEM containing 10% FBS in the indicated conditions for 2 days before being infected with adenovirus or adding COL^{pep} or other treatments. COL^{pep} treatment involved culture for 48 h on dishes that were pre-coated with 2 μ g/ml COL^{pep} or GPP10 control peptide. IL-1 β (10 ng/ml) treatment was conducted for the indicated time. The cells were treated with the indicated concentration of 5-ASA (or 10 μ M 5-ASA) or 5-ASA vehicle (DMSO) for 24–48 h. Rosiglitazone (10 μ M; R2408, Sigma Aldrich) treatment was conducted for 24–48 h.

Western blotting analysis

Articular chondrocytes were lysed with lysis buffer (50 mM Tris-HCl, pH 8.0, 150 mM NaCl, 0.5% deoxycholate acid, and 1% NP-40) containing protease and phosphatase inhibitors. Antibodies against the following proteins were used for Western blotting analysis: OSCAR (Cat# PA5-47171; Thermo Fisher Scientific; 1:1000 dilution), MMP3 (Cat# Ab53015; Abcam; 1:1000 dilution), MMP13 (Cat# Ab39012; Abcam; 1:1000 dilution), ADAMT5 (Cat# Ab41037; Abcam; 1:1000

dilution), COL2a1 (Cat# sc52658; Santa Cruz Biotechnology; 1:1000 dilution), ACAN (Cat# Ab3778; Abcam; 1:1000 dilution), SOX9 (Cat# 82630s; Cell Signaling Technology; 1:1000 dilution), p-Syk (Cat# 2711s; Cell Signaling Technology; 1:1000 dilution), Syk (Cat# 13198; Cell Signaling Technology; 1:1000 dilution), p-PLC γ 2 (Cat# 3874 S; Cell Signaling Technology; 1:1000 dilution), PLC γ 2 (Cat# sc407; Santa Cruz Biotechnology; 1:1000 dilution), iNOS (Cat# Ab178945; Abcam; 1:1000 dilution), COX-2 (Cat# 12282; Cell Signaling Technology; 1:1000 dilution), LOX-5 (Cat# 3289; Cell Signaling Technology; 1:1000 dilution), p-p38 (Cat# 9211 L, Cell Signaling Technology, 1:1000 dilution), p38 (Cat# 9212 L, Cell Signaling Technology, 1:1000 dilution), p-JNK1/2 (Cat# 9251 S, Cell Signaling Technology, 1:1000 dilution), JNK1/2 (Cat# 9252 S, Cell Signaling Technology, 1:1000 dilution), p-ERK (Cat# 9101 L, Cell Signaling Technology, 1:1000 dilution), ERK (Cat# 9102 S, Cell Signaling Technology, 1:1000 dilution), p-Ik β (Cat# 9246 S, Cell Signaling Technology, 1:1000 dilution), Ik β (Cat# 9242 S, Cell Signaling Technology, 1:1000 dilution), p-p65 (Cat# 3031 S, Cell Signaling Technology, 1:1000 dilution), p65 (Cat# 8242 S, Cell Signaling Technology, 1:1000 dilution), p-Akt (Cat# 9271, Cell Signaling Technology, 1:1000 dilution) and Akt (Cat# 9272, Cell Signaling Technology, 1:1000 dilution). Antibodies against β -actin (Cat# sc47778; Santa Cruz Biotechnology; 1:1000 dilution) and GAPDH (Cat# sc32233; Santa Cruz Biotechnology; 1:1000 dilution) served as loading controls.

Induced-fit docking

All the docking and scoring calculations were performed using the Schrödinger software suite (Maestro, version 11.8.012). The SDF file of 5-ASA was acquired from the PubChem database. The file was imported into Maestro and arranged for docking using Ligand Preparation. The atomic coordinates of the crystal structure of OSCAR (Protein Data Bank; PDB ID: 5CJB) were saved from the PDB and prepared by eliminating all solvents, adding hydrogens, and minimal minimization using Protein Preparation Wizard. An ionizer was used to produce an ionized state of the three selected candidate compounds at the target pH of 7.0 ± 2.0 . The input for IFD was the prepared low-energy ligand forms. The IFD protocol was processed on the graphical user interface. Namely, Maestro is linked with the Schrödinger software. Receptor sampling and refinement were conducted for residues within 5.0 Å of each ligand for each ligand–protein complex. IFD prime energy-minimizing with side-chain sampling, prediction module, and the backbone of OSCAR was conducted. The entire induced-fit receptor conformations generated with 5-ASA were scored by combining Prime and Glide Score scoring functions.

RNA-seq analysis to identify OSCAR and 5-ASA downstream targets

Chondrocytes cultured for 2 days were infected with 800 MOI Ad-OSCAR for 2 h. They were then cultured with or without 5-ASA (10 μ M) for an additional 24 h. As a control, the chondrocytes were injected with Ad-Control. All cultures were conducted in plates coated with COL^{pep}. IL-1 β was not present in these cultures. Total RNA was extracted and sequencing libraries were prepared according to manufacturer instructions (TruSeq Stranded mRNA Library Prep Kit; Illumina, San Diego, CA, USA). Thus, paired-end sequencing was performed using an Illumina NovaSeq 6000 system according to the provided protocols for 2×100 sequencing. The sequencing quality of the FASTQ raw files was assessed by using FastQC. The RNA sequencing reads were trimmed by BBDuk and aligned to the GRCh38 genome reference by using STAR v2.7.1a. Raw read counts were obtained by RSEM v.1.3.1. The raw and processed RNA-seq data are available from the Gene Expression Omnibus (GEO) database (accession number GSE207056). The DEGs for OSCAR and 5-ASA were determined by comparing the Ad-Control chondrocytes to the untreated Ad-OSCAR-infected chondrocytes and the 5-ASA-treated Ad-OSCAR-infected chondrocytes, respectively. The differential expression analysis was performed by using DESeq2, and

the Benjamini-Hochberg method⁶⁶ was used for multiple test correction. Since OSCAR and 5-ASA have different ranges of gene expression regulation, we used alternative cut-off criteria to select the DEGs, namely, $|\log_2FC| > 1.5$ and $FDR < 0.05$ for OSCAR and $|FC| > 1.5$ and p -value < 0.05 for 5-ASA. The annotated human genes were mapped to mouse genes by using MGI orthology information. Enrichment factor (EF) was measured by calculating the overlap score ratio of actual value against expected value and significance was measured by using the hypergeometric test. Network analysis was conducted, with the pathways being grouped with K-means clustering. The PPI network was collected from the STRING database v.11.0⁶⁷. Networks were visualized by Cytoscape v.3.8 software⁶⁸.

CMap analysis

Potentially important 5-ASA targets were also identified by using the CMap dataset (L1000), which provides the transcriptome profiles after treatment with 20413 small molecules⁶⁹. We screened this dataset for drugs that mimic 5-ASA by calculating the Jaccard index between the FlipDEGs and the 100 most up/downregulated genes in each drug profile. Only profiles with high-quality and FDA-approved drugs were used. Since many drugs had multiple profiles due to the use of different doses, harvesting times, and cell lines, a hypergeometric test was conducted with the top 10% of all Jaccard index scores. The target scores reflect the enrichment factor of drug–target interactions in the screened 5-ASA-mimicking drugs compared to the others. The Drug-Target interactions were collected from seven public databases, namely, ChEMBL, DGIdb, DrugBank, IUPHAR, KEGG, PharmGKB, and DrugCentral.

Immunofluorescence analysis

Normal murine chondrocytes incubated with COL^{pep}, IL-1 β , and/or 5-ASA were subjected to immunofluorescence staining of COX-2 (Cat# 12282; Cell Signaling Technology; 1:1000 dilution) and DAPI staining (D9542; Sigma Aldrich; 1:1000 dilution) and COX-2 fluorescence intensity was measured by Zeiss LSM 880 with Airyscan.

ELISA for PGE2 and LTB4

Normal murine chondrocytes incubated with COL^{pep}, IL-1 β , and/or 5-ASA were subjected to measure ELISA optical density. We used ELISA kits for PGE2 (R&D systems, #KGE004B) and LTB4 (R&D systems, #KGE006B) according to the manufacturer's instructions.

Generation of bone marrow-derived MSCs, chondrogenesis, and 5-ASA treatment

Primary bone marrow mesenchymal stem cells were isolated from the tibias and femurs of 4–5-week-old male C57BL/6J mice as previously described⁷⁰. The cells were then incubated for 3 weeks in a chondrogenic medium (Hyclone, α -MEM containing 10 μ g/ml insulin, 10 μ g/ml transferrin, and 6 μ g/ml sodium selenite) with or without 5-ASA (10 μ M).

Alcian-Blue staining of cartilage glycosaminoglycans and chondrogenic MSCs

Human knee joint sections were obtained as described above and bone marrow-derived MSCs cultured in the chondrogenic medium were stained with Alcian Blue (B8438; Sigma Aldrich) and photographed with Olympus DP72 charge-coupled device camera (v2.1, Olympus Corporation, Tokyo, Japan). The Alcian-Blue activity in the dishes was also quantified by measuring the absorbance at 630 nm.

Immunohistochemistry

Human knee joint sections obtained as described above were incubated with primary anti-OSCAR antibodies (Cat# SC34235, Santa Cruz

Biotechnology, Inc., Dallas, TX, USA and Biorbyt, LLC, St Louis, USA, 1:200 dilution) at 4 °C overnight, followed by use of a 3,3'-diaminobenzidine peroxidase (DAB; horseradish peroxidase) substrate detection kit (Vector Laboratories, Inc., Burlingame, CA, USA) and counterstaining with hematoxylin. Immunohistochemistry was also conducted with antibodies against MMP3 (Cat# Ab53015; Abcam, Cambridge, MA, USA; 1:50 dilution), MMP13 (Cat# Ab51072; Abcam; 1:25 dilution), Aggrecan (Cat# Ab3778; Abcam; 1:100 dilution), COL2A1 (Cat# MAB8887; Sigma-Aldrich, St Louis, MO, USA; 1:50 dilution), ADAMTS5 (Cat# GTX100332; Genetex, Irvine, CA, USA; 1:200 dilution), SOX9 (Cat# ab185230; Abcam; 1:50 dilution), and PPAR γ (Cat# ab59256; Abcam; 1:25 dilution).

Pellet culture of chondrocytes and treatment with 5-ASA

To isolate bone marrow-derived mesenchymal stem cells (BM-MSCs) from 3- or 4-week-old mice, the following procedure was employed⁷¹. Firstly, the mice were euthanized, and their bodies were disinfected using ethanol. Subsequently, the limbs were carefully dissected, and the skin, muscles, ligaments, and tendons were meticulously removed. The tibia and femur bones were then thoroughly cleansed and transferred to a culture dish containing α -MEM medium, where they were cut into 4–5 pieces. Following a 2-day culture period, the bone pieces were discarded, and the remaining bone marrow was cultured for an additional 5 days. During this time, fusiform-shaped cells emerged by the third day, achieving a confluence level of 70–90% within the subsequent 2 days. The obtained BM-MSCs were further cultured in pellet form within a centrifuge tube, utilizing a cartilage-specific medium. After initiating the pellet culture, 2 μ g/ml of COL^{PEP} was introduced into the medium on the following day. This medium was subjected to treatment with or without 5-ASA. The pellet culture was sustained for a duration of 3 weeks, with regular changes of the culture medium every 2–3 days.

Human chondrocyte spheroid 3D culture

Human chondrocytes were subjected to spheroid culture in a 3D microenvironment with or without 5-ASA. A kit was used for this (Catalog No. SP3D-4650; Sciencell, City, Country). COL^{PEP} was added to the kit medium at 2 μ g/ml at the start of the culture. After 1 week, the diameter of the spheroids was measured with a micro-ruler.

Micro-CT analysis

The right and left hind limbs of 10-week-old male mice that had undergone DMM surgery or sham surgery 10 weeks previously were fixed in 10% formaldehyde, and the femurs and tibias were scanned by *in vivo* micro-CT (Skyscan1176, Bruker microCT, Kontich, Belgium). Supplementary Data 7 shows the micro-CT scanning parameters and reconstruction parameters used to acquire high-quality images. The raw micro-CT data were translated into 2-dimensional cross-sectional gray-scale image slices by using Nrecon (Bruker micro-CT, Kontich, ver.1.6.9.3, Belgium), after which the following structural variables of the trabecular and cortical bones were measured by CT Analyzer (CT-AN ver.1.10.9.0, Bruker, Belgium): the bone volume fraction (BV/TV, %), which is related to the shape of trabeculae. To assess the changes in the tibial SBP and subchondral trabeculae, both the SBP and remaining subchondral trabecular bone regions were manually segmented from the tibia, after which the BV was quantified.

Statistical analyses

The sample size for each experiment was not predetermined. To analyze differences between 2 and >2 groups, students' two-tailed *t*-test, one-way analysis of variance (ANOVA), or two-way ANOVA were conducted, respectively. If ANOVAs were significant, pairwise multiple comparisons were conducted. Data based on the comparison of two samples with a variable measured using an ordinal grading system were analyzed using Sidak's multiple comparisons test. Data based on

ordinal grading systems were analyzed using the non-parametric Mann–Whitney *U* test. Each *n* indicates the number of biologically independent samples, mice per group, or human specimens. The sample size for each experiment was not predetermined. The *P* values are indicated in the figures or in Source Data, and the error bars represent s.e.m. for parametric data and the calculated 95% CIs for nonparametric data. Except where stated, the experiments were not randomized and the investigators were not blinded to allocation during experiments and outcome assessment. Multiple comparisons were performed using Tukey's test, Sidak's test, or Dunn's test with *P* values set at <0.0001. All graphs and statistical analyses were made by using GraphPad Prism (v8.4.3, San Diego, CA, USA). *P*-values are indicated in the figures. The error bars in the figures show S.E.M. or 95% confidence intervals. All data were collected from at least three independent experiments.

Reporting summary

Further information on research design is available in the Nature Portfolio Reporting Summary linked to this article.

Data availability

The data that support the findings of this study are available within the article and its Supplementary Information files. Source data are provided in this paper. RNA-seq data of the Ad-OSCAR-infected and 5-ASA-treated chondrocytes have been deposited in the Gene Expression Omnibus (GEO) under accession number [GSE207056](https://www.ncbi.nlm.nih.gov/geo/query/acc.cgi?acc=GSE207056). The CMap and transcription factor datasets utilized in this study are available at <https://clue.io/> and <https://maayanlab.cloud/Harmonizome/>, respectively. The following figures have associated raw data: Figs. 1b, f, 1i, 3b, d, e, g, 4a–c, e–i, 5c, e, h, 6c, 7a–f; Supplementary Figs. 1c, 2a–c, g, 3a–c, f, h, 5a–g, 6b, d, 7b. For gel Source data, see Supplementary Figure 9. Source data are provided in this paper.

References

1. Hunter, D. J., Schofield, D. & Callander, E. The individual and socioeconomic impact of osteoarthritis. *Nat. Rev. Rheumatol.* **10**, 437–441 (2014).
2. Loeser, R. F., Goldring, S. R., Scanzello, C. R. & Goldring, M. B. Osteoarthritis: a disease of the joint as an organ. *Arthritis Rheum.* **64**, 1697–1707 (2012).
3. Roemer, F. W., Kwok, C. K., Hayashi, D., Felson, D. T. & Guermazi, A. The role of radiography and MRI for eligibility assessment in DMOAD trials of knee OA. *Nat. Rev. Rheumatol.* **14**, 372–380 (2018).
4. Kapoor, M., Martel-Pelletier, J., Lajeunesse, D., Pelletier, J. P. & Fahmi, H. Role of proinflammatory cytokines in the pathophysiology of osteoarthritis. *Nat. Rev. Rheumatol.* **7**, 33–42 (2011).
5. Goldring, M. B. & Otero, M. Inflammation in osteoarthritis. *Curr. Opin. Rheumatol.* **23**, 471–478 (2011).
6. Wang, J. et al. TNF- α and IL-1 β promote a disintegrin-like and metalloprotease with thrombospondin type I motif-5-mediated aggrecan degradation through syndecan-4 in intervertebral disc. *J. Biol. Chem.* **286**, 39738–39749 (2011).
7. Poole, A. R. et al. Proteolysis of the collagen fibril in osteoarthritis. *Biochem. Soc. Symp.* **70**, 115–123 (2003).
8. Aigner, T., Soder, S., Gebhard, P. M., McAlinden, A. & Haag, J. Mechanisms of disease: role of chondrocytes in the pathogenesis of osteoarthritis-structure, chaos and senescence. *Nat. Clin. Pract. Rheumatol.* **3**, 391–399 (2007).
9. Kim, N., Takami, M., Rho, J., Josien, R. & Choi, Y. A novel member of the leukocyte receptor complex regulates osteoclast differentiation. *J. Exp. Med.* **195**, 201–209 (2002).
10. Barrow, A. D. et al. OSCAR is a collagen receptor that costimulates osteoclastogenesis in DAP12-deficient humans and mice. *J. Clin. Invest.* **121**, 3505–3516 (2011).

11. Zhou, L. et al. Structural basis for collagen recognition by the immune receptor OSCAR. *Blood* **127**, 529–537 (2016).
12. Haywood, J. et al. Structural basis of collagen recognition by human osteoclast-associated receptor and design of osteoclastogenesis inhibitors. *Proc. Natl Acad. Sci. USA* **113**, 1038–1043 (2016).
13. Merck, E. et al. OSCAR is an FcRgamma-associated receptor that is expressed by myeloid cells and is involved in antigen presentation and activation of human dendritic cells. *Blood* **104**, 1386–1395 (2004).
14. Park, D. R. et al. Osteoclast-associated receptor blockade prevents articular cartilage destruction via chondrocyte apoptosis regulation. *Nat. Commun.* **11**, 4343 (2020).
15. Kim, G. M., Park, H. & Lee, S. Y. Roles of osteoclast-associated receptor in rheumatoid arthritis and osteoarthritis. *Jt. Bone Spine* **89**, 105400 (2022).
16. Subramanian, S. et al. Characterization of epithelial IL-8 response to inflammatory bowel disease mucosal *E. coli* and its inhibition by mesalamine. *Inflamm. Bowel Dis.* **14**, 162–175 (2008).
17. Feagan, B. G. & Macdonald, J. K. Oral 5-aminosalicylic acid for induction of remission in ulcerative colitis. *Cochrane Database Syst. Rev.* **10**, CD000543 (2012).
18. Glasson, S. S., Blanchet, T. J. & Morris, E. A. The surgical destabilization of the medial meniscus (DMM) model of osteoarthritis in the 129/SvEv mouse. *Osteoarthr. Cartil.* **15**, 1061–1069 (2007).
19. Choi, W. S. et al. The CH25H-CYP7B1-RORalpha axis of cholesterol metabolism regulates osteoarthritis. *Nature* **566**, 254–258 (2019).
20. Choi, W. S. et al. Critical role for arginase II in osteoarthritis pathogenesis. *Ann. Rheum. Dis.* **78**, 421–428 (2019).
21. Jenei-Lanzl, Z., Meurer, A. & Zaucke, F. Interleukin-1beta signaling in osteoarthritis—chondrocytes in focus. *Cell Signal.* **53**, 212–223 (2019).
22. Salinas, C. N., Cole, B. B., Kasko, A. M. & Anseth, K. S. Chondrogenic differentiation potential of human mesenchymal stem cells photoencapsulated within poly(ethylene glycol)-arginine-glycine-aspartic acid-serine thiol-methacrylate mixed-mode networks. *Tissue Eng.* **13**, 1025–1034 (2007).
23. Ducker, G. S. & Rabinowitz, J. D. One-carbon metabolism in health and disease. *Cell Metab.* **25**, 27–42 (2017).
24. Rousseaux, C. et al. Intestinal antiinflammatory effect of 5-aminosalicylic acid is dependent on peroxisome proliferator-activated receptor-gamma. *J. Exp. Med.* **201**, 1205–1215 (2005).
25. Mochizuki, K., Suruga, K., Sakaguchi, N., Takase, S. & Goda, T. Major intestinal coactivator p300 strongly activates peroxisome proliferator-activated receptor in intestinal cell line, Caco-2. *Gene* **291**, 271–277 (2002).
26. Ouyang, Y. et al. Overexpression of SOX9 alleviates the progression of human osteoarthritis in vitro and in vivo. *Drug Des. Dev. Ther.* **13**, 2833–2842 (2019).
27. Li, T. & Chiang, J. Y. Regulation of bile acid and cholesterol metabolism by PPARs. *PPAR Res.* **2009**, 501739 (2009).
28. Chen, H. et al. ATF4 regulates SREBP1c expression to control fatty acids synthesis in 3T3-L1 adipocytes differentiation. *Biochim. Biophys. Acta* **1859**, 1459–1469 (2016).
29. Selvarajah, B. et al. mTORC1 amplifies the ATF4-dependent de novo serine-glycine pathway to supply glycine during TGF-beta(1)-induced collagen biosynthesis. *Sci. Signal.* **12**, eaav3048 (2019).
30. Kilberg, M. S., Shan, J. & Su, N. ATF4-dependent transcription mediates signaling of amino acid limitation. *Trends Endocrinol. Metab.* **20**, 436–443 (2009).
31. Bardot, O., Aldridge, T. C., Latruffe, N. & Green, S. PPAR-RXR heterodimer activates a peroxisome proliferator response element upstream of the bifunctional enzyme gene. *Biochem. Biophys. Res. Commun.* **192**, 37–45 (1993).
32. Kwon, O. S. et al. Connectivity map-based drug repositioning of bortezomib to reverse the metastatic effect of GALNT14 in lung cancer. *Oncogene* **39**, 4567–4580 (2020).
33. Zhu, L. et al. Variants in ALDH1A2 reveal an anti-inflammatory role for retinoic acid and a new class of disease-modifying drugs in osteoarthritis. *Sci. Transl. Med.* **14**, eabm4054 (2022).
34. McAdam, B. F. et al. Effect of regulated expression of human cyclooxygenase isoforms on eicosanoid and isoeicosanoid production in inflammation. *J. Clin. Invest.* **105**, 1473–1482 (2000).
35. Wang, T. et al. Arachidonic acid metabolism and kidney inflammation. *Int. J. Mol. Sci.* **20**, 3683 (2019).
36. Pruzanski, W., Vadas, P., Stefanski, E. & Urowitz, M. B. Phospholipase A2 activity in sera and synovial fluids in rheumatoid arthritis and osteoarthritis. Its possible role as a proinflammatory enzyme. *J. Rheumatol.* **12**, 211–216 (1985).
37. Martel-Pelletier, J., Lajeunesse, D., Reboul, P. & Pelletier, J. P. Therapeutic role of dual inhibitors of 5-LOX and COX, selective and non-selective non-steroidal anti-inflammatory drugs. *Ann. Rheum. Dis.* **62**, 501–509 (2003).
38. Mathis, S., Jala, V. R. & Haribabu, B. Role of leukotriene B4 receptors in rheumatoid arthritis. *Autoimmun. Rev.* **7**, 12–17 (2007).
39. Abramson, S. B., Attur, M., Amin, A. R. & Clancy, R. Nitric oxide and inflammatory mediators in the perpetuation of osteoarthritis. *Curr. Rheumatol. Rep.* **3**, 535–541 (2001).
40. Yang, W. L. & Frucht, H. Activation of the PPAR pathway induces apoptosis and COX-2 inhibition in HT-29 human colon cancer cells. *Carcinogenesis* **22**, 1379–1383 (2001).
41. Yi, J. H., Park, S. W., Brooks, N., Lang, B. T. & Vemuganti, R. PPAR-gamma agonist rosiglitazone is neuroprotective after traumatic brain injury via anti-inflammatory and anti-oxidative mechanisms. *Brain Res.* **1244**, 164–172 (2008).
42. Murphy, J. M. et al. Reduced chondrogenic and adipogenic activity of mesenchymal stem cells from patients with advanced osteoarthritis. *Arthritis Rheum.* **46**, 704–713 (2002).
43. Kim, D. H. et al. PPAR-delta agonist affects adipo-chondrogenic differentiation of human mesenchymal stem cells through the expression of PPAR-gamma. *Regen. Ther.* **15**, 103–111 (2020).
44. Grillet, B. et al. Matrix metalloproteinases in arthritis: towards precision medicine. *Nat. Rev. Rheumatol.* **19**, 363–377 (2023).
45. Roughley, P. J. & Mort, J. S. The role of aggrecan in normal and osteoarthritic cartilage. *J. Exp. Orthop.* **1**, 8 (2014).
46. Chiquet, M. Regulation of extracellular matrix gene expression by mechanical stress. *Matrix Biol.* **18**, 417–426 (1999).
47. Goldring, M. B. The role of the chondrocyte in osteoarthritis. *Arthritis Rheum.* **43**, 1916–1926 (2000).
48. Li, K. et al. Anti-inflammatory and pro-anabolic effects of 5-aminosalicylic acid on human inflammatory osteoarthritis models. *J. Orthop. Transl.* **38**, 106–116 (2023).
49. Sandborn, W. J. Oral 5-ASA therapy in ulcerative colitis: what are the implications of the new formulations? *J. Clin. Gastroenterol.* **42**, 338–344 (2008).
50. Timur, U. T. et al. Chondroprotective actions of selective COX-2 inhibitors in vivo: a systematic review. *Int. J. Mol. Sci.* **21**, 6962 (2020).
51. Nakata, K. et al. Disease-modifying effects of COX-2 selective inhibitors and non-selective NSAIDs in osteoarthritis: a systematic review. *Osteoarthr. Cartil.* **26**, 1263–1273 (2018).
52. Kobayashi, T. et al. Pioglitazone, a peroxisome proliferator-activated receptor gamma agonist, reduces the progression of experimental osteoarthritis in guinea pigs. *Arthritis Rheum.* **52**, 479–487 (2005).
53. Vashghani, F. et al. PPARgamma deficiency results in severe, accelerated osteoarthritis associated with aberrant mTOR signaling in the articular cartilage. *Ann. Rheum. Dis.* **74**, 569–578 (2015).
54. Dubuquoy, L. et al. PPARgamma as a new therapeutic target in inflammatory bowel diseases. *Gut* **55**, 1341–1349 (2006).

55. Bernstein, C. N., Wajda, A. & Blanchard, J. F. The clustering of other chronic inflammatory diseases in inflammatory bowel disease: a population-based study. *Gastroenterology* **129**, 827–836 (2005).
56. Di Paolo, M. C. et al. Sulphasalazine and 5-aminosalicylic acid in long-term treatment of ulcerative colitis: report on tolerance and side-effects. *Dig. Liver Dis.* **33**, 563–569 (2001).
57. Xue, H., Li, J., Xie, H. & Wang, Y. Review of drug repositioning approaches and resources. *Int. J. Biol. Sci.* **14**, 1232–1244 (2018).
58. Bosworth, B. P., Sandborn, W. J., Rubin, D. T. & Harper, J. R. Baseline oral 5-ASA use and efficacy and safety of budesonide foam in patients with ulcerative proctitis and ulcerative proctosigmoiditis: analysis of 2 Phase 3 studies. *Inflamm. Bowel Dis.* **22**, 1881–1886 (2016).
59. Kapadia, R., Yi, J. H. & Vemuganti, R. Mechanisms of anti-inflammatory and neuroprotective actions of PPAR-gamma agonists. *Front. Biosci.* **13**, 1813–1826 (2008).
60. Nobilis, M. et al. High-performance liquid-chromatographic determination of 5-aminosalicylic acid and its metabolites in blood plasma. *J. Chromatogr. A* **1119**, 299–308 (2006).
61. Gardiner, M. D. et al. Transcriptional analysis of micro-dissected articular cartilage in post-traumatic murine osteoarthritis. *Osteoarthritis. Cartil.* **23**, 616–628 (2015).
62. Glasson, S. S., Chambers, M. G., Van Den Berg, W. B. & Little, C. B. The OARS histopathology initiative—recommendations for histological assessments of osteoarthritis in the mouse. *Osteoarthritis. Cartil.* **18**, S17–S23 (2010).
63. van der Kraan, P. M. Factors that influence outcome in experimental osteoarthritis. *Osteoarthritis. Cartil.* **25**, 369–375 (2017).
64. Ma, H. L. et al. Osteoarthritis severity is sex dependent in a surgical mouse model. *Osteoarthritis. Cartil.* **15**, 695–700 (2007).
65. Krenn, V. et al. Synovitis score: discrimination between chronic low-grade and high-grade synovitis. *Histopathology* **49**, 358–364 (2006).
66. Ferreira, J. A. The Benjamini-Hochberg method in the case of discrete test statistics. *Int. J. Biostat.* **3**, Article 11 (2007).
67. Szklarczyk, D. et al. The STRING database in 2017: quality-controlled protein-protein association networks, made broadly accessible. *Nucleic Acids Res.* **45**, D362–D368 (2017).
68. Kohl, M., Wiese, S. & Warscheid, B. Cytoscape: software for visualization and analysis of biological networks. *Methods Mol. Biol.* **696**, 291–303 (2011).
69. Subramanian, A. et al. A Next Generation Connectivity Map: L1000 platform and the first 1,000,000 profiles. *Cell* **171**, 1437–1452.e1417 (2017).
70. Zhao, D. et al. Treatment of early stage osteonecrosis of the femoral head with autologous implantation of bone marrow-derived and cultured mesenchymal stem cells. *Bone* **50**, 325–330 (2012).
71. Ong, S. Y., Dai, H. & Leong, K. W. Inducing hepatic differentiation of human mesenchymal stem cells in pellet culture. *Biomaterials* **27**, 4087–4097 (2006).
- Foundation of Korea (2021R1A2C3003675 and RS-2023-00217798 to S.Y.L.; 2022R11A1A01054308 to J.K.) and by the Korea Basic Science Institute National Research Facilities & Equipment Center grant (2019R1A6C1010020). We would like to thank Yongwon Choi (University of Pennsylvania, USA) for helpful discussions and suggestions.

Author contributions

J.K. performed the experiments, analyzed the data, and co-wrote the paper. J.K., J.S., M.G., G.K., S.Y., S.K., D.H.S., and H.S. performed the in vitro and in vivo experiments. G.R. and W.K. analyzed the RNA-Seq data. H.L. and H.S.K. performed and analyzed the Micro CT data. J.Y.L. interpreted the data and provided scientific discussion. M.C.P. evaluated the human samples. S.Y.L. designed the study, analyzed and interpreted the data, and co-wrote the paper.

Competing interests

The authors declare no competing interests.

Additional information

Supplementary information The online version contains supplementary material available at <https://doi.org/10.1038/s41467-024-45174-6>.

Correspondence and requests for materials should be addressed to Soo Young Lee.

Peer review information *Nature Communications* thanks Francesco Dell’Accio, Tonia Vincent, and the other anonymous reviewer(s) for their contribution to the peer review of this work. A peer review file is available.

Reprints and permissions information is available at <http://www.nature.com/reprints>

Publisher’s note Springer Nature remains neutral with regard to jurisdictional claims in published maps and institutional affiliations.

Open Access This article is licensed under a Creative Commons Attribution 4.0 International License, which permits use, sharing, adaptation, distribution and reproduction in any medium or format, as long as you give appropriate credit to the original author(s) and the source, provide a link to the Creative Commons license, and indicate if changes were made. The images or other third party material in this article are included in the article’s Creative Commons license, unless indicated otherwise in a credit line to the material. If material is not included in the article’s Creative Commons license and your intended use is not permitted by statutory regulation or exceeds the permitted use, you will need to obtain permission directly from the copyright holder. To view a copy of this license, visit <http://creativecommons.org/licenses/by/4.0/>.

© The Author(s) 2024

Acknowledgements

The schematic illustration in the figure was created with BioRender.com. This work was supported by grants from the National Research